Vilniaus universitetas
Fizikos fakultetas
Teorinės fizikos ir astronomijos institutas

Simonas Draukšas

SPHENO IR FLEXIBLESUSY PALYGINIMAS GRIMUS-NEUFELD MODELYJE

Pagrindinių studijų baigiamasis darbas

Fizikos
studijų programa

Studentas	Simonas Draukšas
Leista ginti	(data)
Darbo vadovas	doc. dr. Thomas Gajdosik
Instituto atstovas	prof. Egidijus Anisimovas

Vilnius 2018

Contents

Introduction

Particle physics is a fairly new branch of physics. It started out in the early 20th century and is one of the branches on the edge of modern research. Despite huge achievements, there still are enormous tasks to be done: dark matter and dark energy, super symmetry and string theory, quantum theory of gravitation, masses of neutrinos, etc. This thesis is concerned with the last problem — masses of neutrinos. Not too long ago the neutrinos were thought to be massless, but after confirming neutrino oscillations their masslessness became impossible. The usual Higgs mechanism does not seem to be suitable, since the masses of neutrinos are very small as compared to other particles and that implies unnaturally small couplings. In addition, right-handed neutrinos are decoupled from the Standard Model and not observed, making it hard to know if the Higgs mechanism is in effect. In general, there are many models trying to solve not only neutrino related problems, which require a lot of complex computations and the usage of various software becomes mandatory if one wants to look at the phenomenology of the model. In the thesis we introduce a plausible solution to the neutrino mass problem, the Grimus-Neufeld model [1], and look at its implementation using software.

The goal of the thesis is to finish the implementation of the Grimus-Neufeld model started in the coursework [2] in `FlexibleSUSY` [3, 4, 5, 6] and `SPheno` [7, 8], and to perform a comparison of the two software packages in various aspects of the model.

In Sec. 1 the necessary theoretical background is introduced: basic concepts in particle physics and the elements of the Grimus-Neufeld model. We also describe the used software packages more generally. In Sec. 2 we finish implementing the model and briefly describe the process of doing parameter scans. In Sec. 3 scans in various parts of the model are performed and the packages are compared.

1 Review of theory and software

In this section we introduce the relevant topics for understanding the thesis. The larger part is dedicated to physics: concept of symmetries, properties of mass terms in the Lagrangian, a brief review of the Standard Model, and a detailed description of the Grimus-Neufeld model, which is the core component of the thesis. Sections about symmetries, the Standard Model, and the Grimus-Neufeld model are mostly based on the previously written coursework [2] with some minor additions as well as some cuts. In the non-physical part the software packages that were used are briefly introduced.

1.1 Symmetries

With the help of the mathematical formalism of group theory symmetries play a key role in particle physics. In general, an object is considered to be symmetric if it remains unchanged, or invariant, under some transformation. In our case that object is the Lagrangian. Via Noether's theorem symmetries imply conservation laws and vice versa. The four fundamental forces are described using gauge fields, which are symmetric under transformations of a specific group. Therefore, we begin by providing some detail and necessary concepts of symmetries in particle physics.

In essence, there are two types of continuous symmetries: global and local. Global means that the transformation is uniform and affects every point in spacetime equally, while local transformations smoothly vary from point to point. Since local transformations are a bit complicated we first describe the global case.

While the following subsections about symmetries are based on [2], the textbook material was originally taken from [9] and [10].

1.1.1 Global symmetries

As an intuitive explanation for introducing such symmetries one could think about a global shift in spacetime. Due to such a shift the physics do not change. Quite similarly, in particle physics a phase shift is considered for a Lagrangian of a massive complex scalar (boson):

$$-\mathcal{L} = \partial_\mu \phi^\dagger \partial^\mu \phi + m^2 \phi^\dagger \phi. \tag{1.1.1}$$

Here, and everywhere else, $\mathcal{L}$ is the Lagrangian density, but will be referred to as the Lagrangian for simplicity. ϕ is the complex scalar field, the first term in the Lagrangian is the kinetic term and the second term is the potential term. Consider the transformation:

$$\begin{aligned} \phi' &\to \mathrm{e}^{\mathrm{i}\alpha}\phi, \\ \phi'^\dagger &\to \phi^\dagger \mathrm{e}^{-\mathrm{i}\alpha}. \end{aligned} \tag{1.1.2}$$

α is an arbitrary phase. This transformation is a $U(1)$ transformation, because $\mathrm{e}^{\mathrm{i}\alpha}$ is an element of the group of all 1×1 unitary matrices. We can easily see that under this transformation the

Lagrangian does not change:

$$-\mathcal{L}' = \partial_\mu \phi'^\dagger \partial^\mu \phi' + m^2 \phi'^\dagger \phi' = -\mathcal{L}. \tag{1.1.3}$$

We now consider changing the potential term:

$$m^2 \phi^\dagger \phi \to \lambda \left(\phi^\dagger \phi - \frac{v^2}{2} \right)^2 . \tag{1.1.4}$$

Here v and λ are real constants. With this potential the Lagrangian is still invariant under $U(1)$ transformations, but now the potential also has an extremum at $|\phi|^2 = v^2$, which is a minimum. Expanding the fields around the minimum we get:

$$\phi = \frac{1}{\sqrt{2}}(v + \rho + \mathrm{i}\sigma) \tag{1.1.5}$$

Here ρ and σ are both real fields that represent the two degrees of freedom. Plugging in equation (1.1.5) into Eq.(1.1.1) with the new potential and expanding we get:

$$-\mathcal{L} = \left(\frac{1}{2} \partial_\mu \rho^\dagger \partial^\mu \rho + \frac{1}{2} \partial_\mu \sigma^\dagger \partial^\mu \sigma \right) + \frac{1}{4} \lambda \left(\rho^4 + 4v\rho^3 + 4v^2\rho^2 + 4v\rho\sigma^2 + \rho^2\sigma^2 + \sigma^4 \right). \tag{1.1.6}$$

The procedure of expanding fields around the minimum might seem to not have a very clear reason at this point. First of all, the altered potential has the famous „Mexican hat“ form and there is a circle with the radius v, which marks the minimum of the potential. v is also known as the Vacuum Expectation Value (VEV). Secondly, the Lagrangian no longer has an obvious $U(1)$ symmetry, though it is still there, therefore, this procedure is called the spontaneous symmetry breaking. With this procedure we acquire a massive field ρ, we see that from the bilinear term $\lambda v^2 \rho^2$. We also get a massless field σ, because terms of higher powers than 2 in ρ and σ describe interactions. It turns out that by breaking a global symmetry of some group we always get an amount of massless particles equal to the number of vacuum non-annihilating generators of that group. Such particles are called Goldstone bosons and the statement is the Goldstone theorem. Proofs and derivations of the theorem can be found in [11] and [12].

1.1.2 Local symmetries

Requiring the Lagrangian to be invariant under local symmetries is a bit strange at first sight, but the benefits are immense. We use a similar example to that of the global case. We consider the Dirac Lagrangian for a fermion field ψ:

$$\mathcal{L} = \bar{\psi} \left(\mathrm{i}\gamma^\mu \partial_\mu - m \right) \psi \tag{1.1.7}$$

and use the transformation:

$$\psi' \to \mathrm{e}^{\mathrm{i}\alpha(x)} \psi. \tag{1.1.8}$$

Here $\bar{\psi} = \psi^\dagger \gamma^0$, γ^μ are the Dirac gamma matrices and α is a function of the 4 spacetime components x. Unfortunately, the Lagrangian is not symmetric under this transformation since we get an extra term:

$$\mathcal{L}' = \bar{\psi} \left(\mathrm{i}\gamma^\mu \partial_\mu - m \right) \psi - \bar{\psi} \gamma^\mu \psi \partial_\mu \alpha \left(x \right). \tag{1.1.9}$$

In order to cancel out this term the covariant derivative together with the additional vector field A_μ is introduced. The vector field is such that under local $U(1)$ transformation it transforms in the following way:

$$A_\mu \to A_\mu - \frac{1}{q}\partial_\mu \alpha\left(x\right). \tag{1.1.10}$$

The covariant derivative is:

$$D_\mu = \partial_\mu + \mathrm{i}qA_\mu. \tag{1.1.11}$$

Here q is the charge that couples ψ to the field A_μ. With these changes we get the new Lagrangian which has the same form as the Lagrangian we started with and is invariant under local $U(1)$ transformations:

$$\mathcal{L}_D = \bar{\psi}\left(\mathrm{i}\gamma^\mu D_\mu - m\right)\psi. \tag{1.1.12}$$

Introduction of covariant derivatives may seem strange at this point, but they do have a deeper meaning which is geometrical as well as physical. Covariant derivatives transform linearly, because they have connection terms (or gauge fields) that cancel non-linear terms. For the physical part, by making the symmetries local or „gauging“ them we have made the jump from inertial frames of reference to non-inertial frames. Also, with the introduction of a covariant derivative we have made the *form* of the equation invariant with respect to the frames of reference. By making spacetime symmetries, which are *external*, local we allow the curvature of spacetime. In analogy, by making *internal* symmetries, such as $U(1)$, local we also allow non-inertial reference frames in the additional space of $U(1)$. Geometrically we introduce connection terms (Christoffel symbols) in the derivative and in this way form a covariant derivative, physically we introduce gauge fields, A_μ in this case. Gauge fields play the role of force carrying particles and therefore it makes sense that these fields change the geodesics just like the connection terms.

However, the new gauge field still has a problem: there is no kinetic term, which means that the field is a constant background and does not change a thing. To account for this, we introduce the strength tensor:

$$F^{\mu\nu} = \frac{\mathrm{i}}{q}\left[D^\mu, D^\nu\right] = \partial^\mu A^\nu - \partial^\nu A^\mu. \tag{1.1.13}$$

Using the strength tensor to form the kinetic term we get the final Lagrangian:

$$\mathcal{L} = \bar{\psi}\left(i\gamma^\mu D_\mu - m\right)\psi - \frac{1}{4}F_{\mu\nu}F^{\mu\nu}. \tag{1.1.14}$$

By requiring the Lagrangian to be invariant under local symmetry transformations we were forced to introduce the field A_μ. With this new field we get the Lagrangian of electromagnetism. As briefly mentioned above, gauge fields represent force carrying particles and so A_μ is the photon. We also easily see that A_μ is massless since there are no terms bilinear in A_μ. Theories that generate forces by specifying a Lie Group are called Gauge Theories or Yang-Mills Theories.

As in the case of global symmetries, we also want to break the local symmetry and observe the results. For the sake of simplicity, we now switch to the Lagrangian of a complex scalar:

$$\mathcal{L} = -\left[\left(\partial^\mu - \mathrm{i}qA^\mu\right)\phi^\dagger\right]\left[\left(\partial_\mu + \mathrm{i}qA_\mu\right)\phi\right] - \frac{1}{4}F_{\mu\nu}F^{\mu\nu} - V\left(\phi^\dagger, \phi\right). \tag{1.1.15}$$

Here the potential $V\left(\phi^\dagger, \phi\right)$ is of the „Mexican hat“ form in Eq.(1.1.4). Analogically to global symmetries we write the field around its minimum:

$$\phi = \frac{1}{\sqrt{2}}\left(v + h(x)\right). \tag{1.1.16}$$

Once again v is the Vacuum Expectation Value and $h(x)$ is the perturbation. Both the VEV and $h(x)$ are real, because we are able to choose $\mathrm{e}^{\mathrm{i}\alpha(x)}$ in such a way that this holds. Choosing a specific $\mathrm{e}^{\mathrm{i}\alpha(x)}$, or more generally a specific gauge transformation, is referred to as „gauge fixing“. We get:

$$\begin{aligned}\mathcal{L} = &-\frac{1}{2}\left[\left(\partial^\mu - \mathrm{i}qA^\mu\right)(v+h)\right]\left[\left(\partial_\mu + \mathrm{i}qA_\mu\right)(v+h)\right] - \frac{1}{4}F_{\mu\nu}F^{\mu\nu} - \\ &-\frac{1}{4}\lambda\left[(v+h)(v+h) - v^2\right]^2.\end{aligned} \tag{1.1.17}$$

The sign difference in covariant derivatives is of geometrical meaning which can be found in [10]. Skipping the tedious expansion we acquire:

$$\mathcal{L} = -\frac{1}{2}\partial^\mu h \partial_\mu h - \frac{1}{4}4\lambda v^2 h^2 - \frac{1}{4}F^{\mu\nu}F_{\mu\nu} - \frac{1}{2}q^2v^2A^2 + \mathcal{L}_{interactions}. \tag{1.1.18}$$

By analysing the new Lagrangian we can see that we have a real massive scalar field h and our massless force carrying particle gained mass. Before symmetry breaking we had a complex scalar field and a massless gauge field. One degree of freedom from the complex scalar turned into the longitudinal polarisation of A_μ.

By breaking global symmetries we get massless Goldstone bosons and by breaking local symmetries gauge fields acquire masses and get longitudinal polarisations. It is worth to mention, that in the case of local symmetry breaking we get as many masses for the gauge fields as we would have gotten Goldstone bosons if we were to break global symmetries. „Would-be Goldstone bosons“ are absorbed into gauge fields to give masses.

1.1.3 Electroweak symmetry breaking

In this next and final part on symmetries we use local symmetry breaking to break the electroweak symmetry and get massive gauge fields for the weak force while keeping the photon of electromagnetism massless. This section also introduces a Higgs doublet. With foresight it can be said that Higgs doublets are one of the essential parts in the upcoming discussion of the Grimus-Neufeld model. In this section we also follow [9] with some minor changes and comments.

We first begin by motivating our choices. Our goal is to break some specific symmetry in such a way that we end up with 3 massive bosons, namely $W^\pm$ and Z bosons, and the massless photon. As a result, the final symmetry we are left with has to be $U(1)$. This particular set up is already a hint to the Standard Model which is briefly introduced later on. To get this outcome we need 3 „would-be Goldstone bosons“ to be absorbed into 3 massless bosons, therefore we need to break 3 generators. One simple and familiar group with 3 generators is $SU(2)$. Since the final Lagrangian is invariant under $U(1)$, our Lagrangian before symmetry breaking is invariant

under $SU(2) \otimes U(1)$. At this point we also require a complex electroweak Higgs doublet. This doublet holds 4 degrees of freedom. One of them is to become the scalar Higgs, while the other 3 are to be absorbed into the masses of $W^{\pm}$ and Z.

First of all, we need to construct the covariant derivative for the Higgs doublet. In the very same way as we did in Sec.1.1.2 we form the covariant derivative by adding gauge fields that interact with the Higgs, i.e. have non-zero charges of a particular group. We also expand gauge fields in terms of their generators, as an example:

$$A^{\mu} = A^{\mu}_{a} T^{a}. \tag{1.1.19}$$

Here T^a are the generators, A^{μ} is some gauge field which is described by a matrix. By doing this expansion we start treating A^{μ}_{a} as individual fields. Generators of the $SU(2)$ group are the Pauli matrices:

$$T^{a} = \frac{1}{2}\sigma^{a} \tag{1.1.20}$$

and the generator of $U(1)$ is:

$$Y = y_H \begin{pmatrix} 1 & 0 \\ 0 & 1 \end{pmatrix}, \tag{1.1.21}$$

here y_H is the hypercharge. In this case the Higgs doublet has $y_H = -\frac{1}{2}$ assigned. We are now ready to write down the covariant derivative. Keep in mind that now we are not dealing with a simple complex scalar, but with a doublet, therefore we have an additional index i.

$$\left(D_{\mu}\phi\right)_{i} = \partial_{\mu}\phi_{i} - \mathrm{i}\left[g_2 W^{a}_{\mu} T^{a} + g_1 B_{\mu} Y\right]_{ij} \phi_{j}. \tag{1.1.22}$$

Here summation over a, as well as j, is still assumed, but since these are not Lorentz indices it does not really matter if both of the indices are raised or lowered. g_1 and g_2 are the appropriate coupling constants. Already by the usage of generators we can tell that W^{a}_{μ} are the $SU(2)$ gauge fields while B_{μ} is a $U(1)$ field. Since we know the generators we can easily write down the full covariant derivative in matrix form:

$$D_{\mu}\phi \doteq \begin{pmatrix} D_{\mu}\phi_1 \\ D_{\mu}\phi_2 \end{pmatrix} = \begin{pmatrix} \partial_{\mu}\phi_1 + \frac{\mathrm{i}}{2}\left(g_2 W^{3}_{\mu} - g_1 B_{\mu}\right)\phi_1 + \frac{\mathrm{i}g_2}{2}\left(W^{1}_{\mu} - iW^{2}_{\mu}\right)\phi_2 \\ \partial_{\mu}\phi_2 + \frac{\mathrm{i}g_2}{2}\left(W^{1}_{\mu} + \mathrm{i}W^{2}_{\mu}\right)\phi_1 - \frac{\mathrm{i}}{2}\left(g_2 W^{3}_{\mu} + g_1 B_{\mu}\right)\phi_2 \end{pmatrix}. \tag{1.1.23}$$

The Lagrangian has to have kinetic as well as potential terms:

$$\mathcal{L}_{\phi} = -(D_{\mu}\phi_i)^{\dagger}(D^{\mu}\phi_i) - V(\phi^{\dagger}, \phi). \tag{1.1.24}$$

We also assume the potential to have the same form as in Eq.(1.1.4):

$$V(\phi^{\dagger}, \phi) = \lambda\left(\phi^{\dagger}\phi - \frac{v^2}{2}\right)^2. \tag{1.1.25}$$

With $\lambda > 0$ the minimum is at:

$$|\phi| = \frac{v}{\sqrt{2}}. \tag{1.1.26}$$

Just like we chose our gauge to be real when breaking the local $U(1)$ symmetry, in a similar fashion we now choose the doublet to be:

$$\phi(x) = \frac{1}{\sqrt{2}} \begin{pmatrix} v + h(x) \\ 0 \end{pmatrix}. \tag{1.1.27}$$

This particular choice is called the unitary gauge and it was first introduced by S. Weinberg [13, 14]. Now we plug Eq.(1.1.27) into the Lagrangian. Since we are mostly concerned with mass terms we only write down the relevant part:

$$\mathcal{L}_m = -\frac{1}{8} \begin{pmatrix} v & 0 \end{pmatrix} \begin{pmatrix} g_2 W_\mu^3 - g_1 B_\mu & g_2 \left(W_\mu^1 - \mathrm{i} W_\mu^2 \right) \\ g_2 \left(W_\mu^1 + \mathrm{i} W_\mu^2 \right) & -g_2 W_\mu^3 - g_1 B_\mu \end{pmatrix}^2 \begin{pmatrix} v \\ 0 \end{pmatrix}. \tag{1.1.28}$$

We multiply and get:

$$\mathcal{L}_m = -\frac{1}{8} v^2 \left[g_2^2 |W^3|^2 + g_1^2 |B|^2 - 2 g_1 g_2 W_\mu B^\mu + g_2^2 \left(|W^1|^2 + |W^2|^2 \right) \right]. \tag{1.1.29}$$

Now $\mathcal{L}_m$ can be easily rewritten in a different matrix form:

$$\mathcal{L}_m = -\frac{1}{8} v^2 V_\mu^T \begin{pmatrix} g_2^2 & 0 & 0 & 0 \\ 0 & g_2^2 & 0 & 0 \\ 0 & 0 & g_2^2 & -g_1 g_2 \\ 0 & 0 & -g_1 g_2 & g_1^2 \end{pmatrix} V^\mu. \tag{1.1.30}$$

Here we have defined $V_\mu = \left(W_\mu^1, W_\mu^2, W_\mu^3, B_\mu \right)$. In this form it is even easier to see that $W^{1,2}$ are already in mass eigenstates and that W^3 and B mix. Also, the sub-matrix which mixes W^3 and B has a determinant of zero and, therefore, one of the eigenvalues is 0. In other words we get a massless boson. We now redefine the fields (and normalise them) according to the matrix in Eq.(1.1.28):

$$\begin{aligned} W_\mu^+ &= \frac{1}{\sqrt{2}} \left(W_\mu^1 - \mathrm{i} W_\mu^2 \right), \\ W_\mu^- &= \frac{1}{\sqrt{2}} \left(W_\mu^1 + \mathrm{i} W_\mu^2 \right), \\ Z_\mu &= \cos\theta_W W_\mu^3 - \sin\theta_W B_\mu, \\ A_\mu &= \sin\theta_W W_\mu^3 + \cos\theta_W B_\mu. \end{aligned} \tag{1.1.31}$$

Here θ_W is the Weinberg angle, or the Weak Mixing angle, and is defined as:

$$\tan\theta_W = \frac{g_1}{g_2}. \tag{1.1.32}$$

From the definition of θ_W the expressions for the sine and cosine can be easily derived with the help of a right triangle. Next we turn to the study of the mass terms of gauge fields. To do that we rewrite Eq.(1.1.28) in terms of the new fields:

$$\mathcal{L}_m = -\frac{1}{8} \begin{pmatrix} v & 0 \end{pmatrix} \begin{pmatrix} \sqrt{g_1^2 + g_2^2} Z_\mu & g_2 \sqrt{2} W_\mu^+ \\ g_2 \sqrt{2} W_\mu^- & -\sqrt{g_1^2 + g_2^2} A_\mu \end{pmatrix}^2 \begin{pmatrix} v \\ 0 \end{pmatrix}. \tag{1.1.33}$$

Multiplying everything we get:

$$\mathcal{L}_m = -\frac{v^2}{8}\left(g_1^2 + g_2^2\right) Z_\mu Z^\mu - \frac{v^2 g_2^2}{4} W_\mu^+ W^{-\mu} = -M_W^2 W_\mu^+ W^{-\mu} - \frac{1}{2} M_Z^2 Z_\mu Z^\mu. \tag{1.1.34}$$

The masses are:

$$\begin{aligned} M_W &= \frac{v g_2}{2}, \\ M_Z &= \frac{v\sqrt{g_1^2 + g_2^2}}{2}. \end{aligned} \tag{1.1.35}$$

From these definitions a very nice relation of masses arises:

$$\frac{M_W}{M_Z} = \frac{g_2}{\sqrt{g_1^2 + g_2^2}} = \cos\theta_W. \tag{1.1.36}$$

This concludes the mathematical part of electroweak symmetry breaking and we note a few things. First of all, we have succeeded in retrieving the correct structure of boson masses from local symmetry breaking: we have three massive bosons corresponding to the weak force and one massless boson, which is the photon, corresponding to the electromagnetic force. In addition, the ratio of Z and $W^\pm$ masses allows to determine the weak mixing angle θ_W. Secondly, the theory works in two energy regimes. In the high energy regime we have four massless fields that in essence behave like the photon, after symmetry breaking, in the low energy regime, three of the four fields gain mass. We now move on to discuss mass terms in more detail.

1.2 Mass terms and mass matrices

So far, we have talked quite a bit about masses of particles and mass terms in the Lagrangian. At this point, it is appropriate to discuss a few features of mass terms as well as to introduce the mass matrices and the way to deal with them, since this is important when performing actual computations. This section mostly contains information found in textbooks on Quantum Field Theory (QFT)[15].

We introduce the mass matrix by considering the potential for an arbitrary number of scalar fields and denote the kinetic energy as K and the potential as V:

$$\mathcal{L} = K - V(\phi). \tag{1.2.1}$$

When the potential is at the minimum the first derivative is equal to zero:

$$\left.\frac{\partial V}{\partial \phi_i}\right|_{\phi_{min}} = 0. \tag{1.2.2}$$

From this we get the minimum conditions and we are able to expand the potential around this minimum:

$$V(\phi) = V(\phi_{min}) + \frac{1}{2}\left.\frac{\partial^2 V}{\partial\phi_i \partial\phi_j}\right|_{\phi_{min}} (\phi_i - \phi_{i,min})(\phi_j - \phi_{j,min}) + ... \tag{1.2.3}$$

At this point we redefine the fields in terms of variations around the minimum $\tilde{\phi}_i = \phi_i - \phi_{i,min}$ and see that the second term is bilinear in terms of $\tilde{\phi}$:

$$V(\tilde{\phi}) = V(\phi_{min}) + \frac{1}{2} \left. \frac{\partial^2 V}{\partial\phi_i \partial\phi_j} \right|_{\phi_{min}} \tilde{\phi}_i \tilde{\phi}_j + ... \tag{1.2.4}$$

In turn, this means that the coefficient matrix is the mass matrix containing the mass parameters:

$$M_{ij} = \frac{1}{2} \left. \frac{\partial^2 V}{\partial\phi_i \partial\phi_j} \right|_{\phi_{min}} . \tag{1.2.5}$$

We see that in general the matrix is not diagonal and it is impossible to easily read out the masses. In order to find the masses one needs to diagonalize the mass matrix to get its eigenvalues. As an example, we used scalar fields (spin 0), but the approach stays the same for other kind of fields as well.

However, the mass dimensions of fermionic and bosonic fields differ and in turn the mass dimension of the mass matrix is also different for the respective fields. This comes from dimensional analysis. First of all, in natural units, where $\mathrm{c} = 1$ and $\hbar = 1$, mass has the dimension of energy, which is easily seen from

$$E = m\mathrm{c}^2 \rightarrow E = m. \tag{1.2.6}$$

In these units mass is obviously of dimension $[m] = 1$, velocities are dimensionless $[v] = 0$, which leads to the fact that time and spatial coordinates are of equal dimensions. To find out the mass, or energy, dimension of spacetime we do the following:

$$E = \hbar\omega \rightarrow \frac{2\pi\hbar}{\lambda} \rightarrow \frac{2\pi}{\lambda}. \tag{1.2.7}$$

We see that spatial dimensions are of energy dimension $[\lambda] = -1$. We also note that derivatives with respect to spacetime have energy dimension $[\partial_\mu] = 1$.

To find out the dimensions of fields we are going to analyse the action principle:

$$S = \int \mathrm{d}^4 x \mathcal{L}. \tag{1.2.8}$$

The action S is a power of an exponent in the path integral formulation and it has to be dimensionless. Since $[\mathrm{d}^4 x] = -4$, the Lagrangian density has to have energy dimension $[\mathcal{L}] = 4$, which means that every term in the Lagrangian also has to have dimension equal to 4. Now we only need to analyse the Lagrangians in Eq.(1.1.1) for bosons and Eq.(1.1.7) for fermions, in both cases we take their kinetic terms. For bosonic fields we have

$$[\partial_\mu \phi^\dagger \partial^\mu \phi] = 4 \rightarrow [\phi^\dagger \phi] = 2 \rightarrow [\phi] = 1 \tag{1.2.9}$$

and for fermionic fields

$$[\bar{\psi} \mathrm{i} \gamma^\mu \partial_\mu \psi] = 4 \rightarrow [\bar{\psi}\psi] = 3 \rightarrow [\psi] = \frac{3}{2}. \tag{1.2.10}$$

After these evaluations we see that energy dimensions really do differ for bosonic and fermionic fields. This also leads to the difference in mass matrix dimensions. For boson fields the

eigenvalues of the mass matrix correspond to masses squared, while for fermion fields the eigenvalues correspond to masses themselves.

The mass matrices for bosons differ not only in terms of mass dimensions, they also have different properties as matrices. For example, since the mass term has to be Hermitian, it follows that the mass matrix for bosons also has to be Hermitian:

$$M_{ij}\phi_i^\dagger\phi_j = \left(M_{ij}\phi_i^\dagger\phi_j\right)^\dagger = \phi_j^\dagger\phi_i(M^\dagger)_{ij} \to M_{ij} = (M^\dagger)_{ij}. \tag{1.2.11}$$

Here we used the property:

$$\phi_i^\dagger\phi_j = \left(\phi_i^\dagger\phi_j\right)^\dagger = \phi_j^\dagger\phi_i. \tag{1.2.12}$$

For fermions mass terms arise from the Yukawa coupling to the Higgs, as seen in the discussion about the Grimus-Neufeld model in Sec. 1.4. The important thing is that the Yukawa couplings are arbitrary and do not have to be real, symmetric or Hermitian as the Hermiticity is ensured by having hermitian conjugated terms in the Lagrangian [16]. Yet, in order to have real eigenvalues for the masses one needs to diagonalize a Hermitian matrix. A Hermitian matrix is formed via simple multiplication:

$$\mathcal{M} = M^\dagger M. \tag{1.2.13}$$

This is all well and good in theory but numerical problems arise when calculations need to be done and the energy (mass) dimensions of mass matrices are taken into account. In case of fermions the eigenvalues of matrix in Eq.(1.2.13) correspond to masses squared, which means that numbers grow rapidly and might become too big or too small for the precision used in computers. This problem emerges in Sec. 2.2, where we discuss implementation in `SPheno`, but we move on to introduce the Standard Model.

1.3 The Standard Model

The Standard Model (SM) is the most successful theory and has the best agreement with experimental data [17]. The SM describes electromagnetic, weak and strong interactions while only excluding gravity at this point. The SM also provides fundamental building blocks of our universe, organized in the quarks, the leptons, the gauge bosons, and the Higgs boson. The quark sector contains quarks, which are the constituents of particles such as the proton and neutron. Leptons are the particles that do not interact strongly and in the lepton sector there are neutrinos together with their charged counterparts, such as the electron. The Gauge sector contains particles that mediate forces. There are 8 gluons that mediate the strong force, $W^\pm$ and Z bosons that mediate the weak force and the photon which mediates the electromagnetic force. The newest block is the scalar sector and contains the Higgs boson, which gives masses to the particles. The quark and lepton sectors contain half-integer spin particles (fermions), while the scalar and gauge sectors hold particles with integer spins (bosons). The two former sectors are also arranged into 3 generations. These sectors are summarised in Table 1 and Table 2.

In table 1 we have adopted the notation from [9]. In $SU(3)_C$ and $SU(2)_L$ columns the numbers denote representations, for example, 1 means that the field is a singlet and does not

Table 1. Summary of non-force-carrying particles in the SM [17]

Particle content	Generations	$SU(3)_C$	$SU(2)_L$	$U(1)_Y$
H	1	1	**2**	$-\frac{1}{2}$
ν_R	3	1	1	0
u_R	3	$\bar{\mathbf{3}}$	1	$-\frac{2}{3}$
d_R	3	$\bar{\mathbf{3}}$	1	$\frac{1}{3}$
$\begin{pmatrix}\nu_{\mathrm{L}}\\ e_{\mathrm{L}}\end{pmatrix}$	3	1	**2**	$-\frac{1}{2}$
$\begin{pmatrix}u_{\mathrm{L}}\\ d_{\mathrm{L}}\end{pmatrix}$	3	**3**	**2**	$\frac{1}{6}$

transform, while 2 and 3 denote doublets and triplets. Bold numbers simply denote that the representation's dimension matches the group's dimension and the bar tells about the complex conjugate representation. In case of $U(1)_Y$ column the numbers simply denote the hypercharge.

Table 2. Summary of the gauge sector in the SM [17]. Masses are given in terms of GeV, the electromagnetic charge in multiples of the electron charge.

Gauge sector							
Force	Group	Particles	Mass	EM Charge	Isospin	Hypercharge	Color charge
EM	$U(1)_e$	γ	0	0	0	0	0
Weak	$SU(2)_L$	$W^{\pm}$	80.385	± 1	± 1	0	0
		Z	91.1876	0	0	0	0
Strong	$SU(3)_C$	$8 \times g$	0	0	0	0	$SU(3)$ octet

The Standard Model is a chiral theory, meaning that fields of different handedness couple differently. In the high energy regime the SM Lagrangian is invariant under $SU(3) \otimes SU(2)_L \otimes U(1)_Y$ transformations. The index Y denotes the hypercharge. The index L in $SU(2)_L$ means „Left" and in the high energy regime the electro-weak force couples only to the left-handed fields. This difference is expressed in the mathematical description of particles. Left handed particles are arranged into doublets while right-handed particles are written as singlets:

$$l^{\alpha} = \begin{pmatrix}\nu_{\mathrm{L}}^{\alpha}\\ e_{\mathrm{L}}^{\alpha}\end{pmatrix}, q^{\alpha} = \begin{pmatrix}u_{\mathrm{L}}^{\alpha}\\ d_{\mathrm{L}}^{\alpha}\end{pmatrix}, e_{\mathrm{R}}^{\alpha}, u_{\mathrm{R}}^{\alpha}, d_{\mathrm{R}}^{\alpha}, \quad \alpha = 1, 2, 3. \tag{1.3.1}$$

α is the generation index, l is the left-handed lepton doublet and q is the left-handed quark doublet. $e_{\mathrm{R}}, u_{\mathrm{R}}, d_{\mathrm{R}}$, with the generation index suppressed, are the right-handed charged lepton, up type quark, and down type quark singlets, respectively. The SM does not yet include right-handed neutrinos, because they were thought of as massless, completely decoupled and therefore irrelevant. With the discovery of neutrino oscillations the problem of their mass incorporation is still an open question.

In the low energy regime the electro-weak symmetry $SU(2)_L \otimes U(1)_Y$ is broken into the $U(1)_e$ symmetry of electromagnetism. The e index denotes electric charge. The Higgs mechanism enables right and left handed particles to mix and in this way the weak force is able to affect the right-handed counterparts of left-handed particles.

1.4 The Grimus-Neufeld model

After introducing a more general physics background we are now ready to start discussing the Grimus-Neufeld model. Neutrinos were treated as massless until the discovery of neutrino oscillations, which prove that they are massive. Yet, the source of neutrino masses is not conclusive at this point. Additionally, the masses are very small compared to other particles (e.g., the electron neutrino is lighter than 2 eV, while the electron's mass is ≈ 511 keV [17]), hence why they were held massless. The Grimus-Neufeld model aims to explain neutrino masses and why they are so small. The model uses a couple of extensions and mechanisms beyond the SM, but is not supersymmetric and kept as simple as possible. The extensions are a second Higgs doublet and a single heavy right-handed Majorana neutrino. These extensions use the seesaw mechanism and 1-loop corrections to explain small masses. In the following sections all of these components are discussed in more detail and the discussion is based on the course work [2] with the additional introduction of theoretical and physical parameters.

1.4.1 Additional Higgs doublet

We start by introducing an additional complex scalar Higgs doublet. This additional doublet has identical properties as the one in the SM and now the two of them are denoted as:

$$\phi_a = \begin{pmatrix} \phi_a^+ \\ \phi_a^0 \end{pmatrix}. \tag{1.4.1}$$

Here a can take the values 1 and 2, ϕ^+ denotes the charged part and ϕ^0 denotes the neutral part of the doublet. It is important to form the Higgs potential. We do this by considering that the potential, as well as the Lagrangian, has to be a scalar, operators of mass dimension > 4 are suppressed and that the mass dimension of scalar fields is 1. Having that in mind the most general potential of the Higgs doublets is [18]:

$$V = Y_{a\bar{b}}\phi_{\bar{a}}^\dagger \phi_b + Z_{a\bar{b}c\bar{d}} \left(\phi_{\bar{a}}^\dagger \phi_b\right) \left(\phi_{\bar{c}}^\dagger \phi_d\right). \tag{1.4.2}$$

Parameters of the potential have the following symmetries:

$$\begin{aligned} Y_{a\bar{b}} &= (Y_{\bar{a}b})^\star, \\ Z_{a\bar{b}c\bar{d}} &= Z_{c\bar{d}a\bar{b}} = (Z_{\bar{a}b\bar{c}d})^\star. \end{aligned} \tag{1.4.3}$$

This potential is invariant under $SU(2)$ and $U(1)$ gauge transformations:

$$\phi_a \to \phi_a' = \exp\left[\mathrm{i} y_\phi \phi_B + \frac{\mathrm{i}}{2}\sigma^k \phi_W^k\right]\phi_a. \tag{1.4.4}$$

Here y_ϕ is the hypercharge generator, σ^k are the Pauli matrices, ϕ_B and ϕ_W are the gauge parameters of $U(1)_Y$ and $SU(2)_L$, respectively. Hypercharge $y_\phi = \frac{1}{2}$ is assigned to the doublets.

The potential is also invariant under the Higgs doublet symmetry:

$$\phi_a \to \phi'_a = U_{a\bar{b}}\phi_b \text{ with } U_{a\bar{b}} \in U(2). \tag{1.4.5}$$

This Higgs doublet symmetry is valid if the parameters transform as tensors:

$$Y_{a\bar{b}} = U_{a\bar{c}}Y_{c\bar{d}}U^\dagger_{d\bar{b}} \text{ and } Z_{a\bar{b}c\bar{d}} = U_{a\bar{e}}U_{\bar{b}f}Z_{e\bar{f}g\bar{h}}U^\dagger_{\bar{g}c}U^\dagger_{h\bar{d}}. \tag{1.4.6}$$

Under electroweak symmetry breaking Higgs doublets acquire VEVs and give mass to particles. In general, both of the doublets can have different VEVs that have the constraint:

$$v_{SM} = \sqrt{v_1^2 + v_2^2}. \tag{1.4.7}$$

Yet, in our case we choose a basis where only one of the doublets acquires a non-zero VEV:

$$v_1 = v_{SM} = v \text{ and } v_2 = 0. \tag{1.4.8}$$

This particular basis is called the Higgs basis. In this basis we rewrite our doublets and leave the „would-be-Goldstone“ bosons without rotating them away:

$$H_1 = \frac{1}{\sqrt{2}}\begin{pmatrix} G_r^+ + \mathrm{i}G_i^+ \\ v + h + \mathrm{i}G^0 \end{pmatrix} \text{ and } H_2 = \frac{1}{\sqrt{2}}\begin{pmatrix} H_r^+ + \mathrm{i}H_i^+ \\ H_r^0 + \mathrm{i}H_i^0 \end{pmatrix}. \tag{1.4.9}$$

Here we wrote all of the Goldstones in the first doublet. At this point, we can say that the two complex scalar doublets have 8 degrees of freedom and according to Goldstone's theorem we are breaking the $SU(2)$ symmetry which has 3 generators, hence the number of massless gauge bosons gaining mass in our case. In SM we had only one doublet and only one massive scalar boson remained, now we have two doublets and 5 massive non-gauge bosons remain. In other words, the first doublet is responsible for the „would-be-Goldstone“ bosons, but since we have an additional doublet there are four more physical Higgses: A, H and $H^\pm$. By assigning a zero VEV to the second doublet we are able to distinguish doublets and we are also fixing the Higgs doublet symmetry of the potential to a rephasing symmetry [18]:

$$H_1 \to H'_1 = H_1 \text{ and } H_2 \to H'_2 = e^{\mathrm{i}\theta_{23}}H_2. \tag{1.4.10}$$

After going to a different basis the coefficients also transform and are functions of the old coefficients. We will explicitly name the coefficients later on.

Kinetic terms of the Higgs doublets are assumed and will not be discussed, because they are not relevant to the work.

At this point the purpose of an additional doublet might and should be unclear, but this is resolved after discussing the Majorana neutrino.

1.4.2 Heavy Majorana neutrino

As mentioned previously the model has a heavy neutrino, which is chosen to be a Majorana particle. We note that these particles have a single fermionic degree of freedom since we want the least amount of degrees of freedom possible to keep things simple. We incorporate the Majorana neutrino and add the Majorana mass term:

$$\mathcal{L}_M = -\frac{1}{2} M_{\mathrm{R}} \bar{N}_R N_R^{(\bar{c})} + h.c. = \frac{1}{2} M_R \bar{N}_{\mathrm{R}} \mathcal{C} \bar{N}_{\mathrm{R}}^T + h.c. \tag{1.4.11}$$

Here N_{R} is the right chiral projection of the Majorana field N, $\mathcal{C}$ is the charge conjugation matrix. Details about Majorana particles and $\mathcal{C}$ can be found in [2], [9], and [19]. Here we have only used this definition:

$$N^{(\bar{c})} = \gamma^0 \mathcal{C} N^\star. \tag{1.4.12}$$

It is important to note, that by writing the mass term in this way we are choosing only the right-handed part of N to couple to the neutral fermions. The SM is a left chiral theory and without Yukawa couplings right-handed particles would completely decouple. This is emphasised in following sections.

By using the Majorana constraint it is possible to rewrite this Majorana mass term like a Dirac mass term:

$$\begin{aligned} \mathcal{L}_M = \frac{1}{2} M_{\mathrm{R}} \bar{N}_{\mathrm{R}} \mathcal{C} \bar{N}_{\mathrm{R}}^T + h.c. = -\frac{1}{2} M_{\mathrm{R}} \bar{N}_{\mathrm{R}} N_{\mathrm{R}} + h.c. = \\ - \frac{1}{2} M_{\mathrm{R}} \left(\bar{N} P_{\mathrm{L}} N + \bar{N} P_{\mathrm{R}} N \right) = -\frac{1}{2} M_{\mathrm{R}} \bar{N} N. \end{aligned} \tag{1.4.13}$$

Here $P_{\mathrm{L},R}$ are the projection operators that give the left-handed or right-handed part of a spinor:

$$P_{\mathrm{L},R} = 1 \mp \gamma^5 \text{ with } \gamma^5 = \gamma^0 \gamma^1 \gamma^2 \gamma^3. \tag{1.4.14}$$

One last thing to say before moving on to the actual interplay of the mentioned elements is the necessity of a heavy neutrino. Phenomenologically we do not observe this neutrino, because it is heavy and beyond our energy scale. In terms of theory, this heavy neutrino is integrated out and gives an effective description. The big mass of a Majorana neutrino is one of the key factors in the seesaw mechanism to which we now turn.

1.4.3 Seesaw mechanism

The seesaw mechanism works by coupling a heavy particle to the presumably light particles, acquiring the mass matrix and then diagonalizing it. We start by writing down the relevant terms from the Lagrangian:

$$-\mathcal{L}_{M+D} = \frac{1}{2} M_{\mathrm{R}} \bar{N} P_{\mathrm{L}} N^{(\bar{c})} + \frac{1}{2} M_{\mathrm{R}} \bar{N}^{(\bar{c})} P_{\mathrm{R}} N + \left(\bar{\nu}_{\mathrm{L}j} (M_{\mathrm{D}})_j P_{\mathrm{R}} N + \bar{N} (M_{\mathrm{D}}^\dagger)_k P_{\mathrm{L}} \nu_{\mathrm{L}k} \right). \tag{1.4.15}$$

The first two terms essentially are the Majorana mass term from Eq.(1.4.13), while the second term comes from the coupling of left-handed neutrinos to the Majorana neutrino. With foresight, it can be mentioned that the second term is from the Yukawa couplings, that couple the Higgs

to left-handed and right-handed fermions and gives a Dirac mass term, when the Higgs acquires a vacuum expectation value. $(M_{\rm D})_k$ come from Yukawas and the VEV and are the mass parameters of light neutrino flavour states. We also state that the Majorana neutrino couples to the superposition of light neutrinos and because of this coupling we will be able to obtain the neutrino mixing matrix and their masses. To get the mixing matrix we rewrite our spinors in Weyl (chiral) basis in terms of two component Weyl spinors. The Majorana field is:

$$N = \begin{pmatrix} \chi_N \\ \bar{\epsilon}\chi_N^\star \end{pmatrix} \tag{1.4.16}$$

and the chiral neutrino fields are:

$$\nu_k = \begin{pmatrix} \chi_k \\ 0 \end{pmatrix} \text{ and } \bar{\nu}_k = \begin{pmatrix} 0 & \chi_k^\dagger \end{pmatrix}. \tag{1.4.17}$$

Here $\epsilon/\bar{\epsilon}$ is the spinor metric defining the Lorentz invariant product of two left/right chiral spinors. In this basis the charge conjugation matrix is given by:

$$\gamma^0\mathcal{C} = \eta_C\gamma^2 = \begin{pmatrix} 0 & \mathrm{i}\sigma^2 \\ \mathrm{i}\bar{\sigma}^2 & 0 \end{pmatrix} =: \begin{pmatrix} 0 & \epsilon \\ \bar{\epsilon} & 0 \end{pmatrix}. \tag{1.4.18}$$

We can choose the phase η_C so that the spinor metrics ϵ are real. In Weyl basis we choose $\eta_C = \pm\mathrm{i}$ and get $\bar{\epsilon} = -\epsilon$, from antisymmetry relation $\epsilon^T = -\epsilon$ we also get $\bar{\epsilon}^T = \epsilon$ and $\epsilon\cdot\epsilon = -1$. We note that we write ϵ instead of $\mathrm{i}\sigma^2$ simply because we have chosen a specific representation. With this we can check that N fulfils the Majorana condition with $N^{(\bar{c})}$:

$$N^{(\bar{c})} = \begin{pmatrix} 0 & \epsilon \\ \bar{\epsilon} & 0 \end{pmatrix}\begin{pmatrix} \chi_N^\star \\ \bar{\epsilon}\chi_N \end{pmatrix} = \begin{pmatrix} \epsilon\bar{\epsilon}\chi_N \\ \bar{\epsilon}\chi_N^\star \end{pmatrix} = \begin{pmatrix} \chi_N \\ \bar{\epsilon}\chi_N^\star \end{pmatrix} = N. \tag{1.4.19}$$

We can now expand the neutral fermion mass terms in Eq.(1.4.15):

$$\begin{aligned} -\mathcal{L}_{M+D} &= \frac{1}{2}M_{\rm R}\left(\chi_N^T\epsilon\chi_N + 0\right) + \frac{1}{2}M_{\rm R}\left(0 + \chi_N^\dagger\bar{\epsilon}\chi_N^\star\right) \\ &\quad + \left(0 + \chi_j^\dagger(M_{\rm D})_j\bar{\epsilon}\chi_N^\star + \chi_N^T\epsilon(M_{\rm D}^\dagger)_k\chi_k + 0\right) \\ &= \frac{1}{2}\left(M_{\rm R}\chi_N^T\epsilon\chi_N + (M_{\rm D}^\star)_k\chi_N^T\epsilon\chi_k + (M_{\rm D}^\star)_j\,\chi_j^T\epsilon\chi_N\right) \\ &\quad + \frac{1}{2}\left(M_{\rm R}\chi_N^\dagger\bar{\epsilon}\chi_N^\star + (M_{\rm D})_k\,\chi_N^\dagger\bar{\epsilon}\chi_k^\star + (M_{\rm D})_j\,\chi_j^\dagger\bar{\epsilon}\chi_N^\star\right) \\ &= \frac{1}{2}\left[M_{\rm R}(\chi_N\chi_N) + (M_{\rm D}^\star)_k(\chi_N\chi_k) + (M_{\rm D}^\star)_j(\chi_j\chi_N)\right] \\ &\quad + \frac{1}{2}\left[M_{\rm R}(\chi_N^\star\chi_N^\star) + (M_{\rm D})_j(\chi_j^\star\chi_N^\star) + (M_{\rm D})_k(\chi_N^\star\chi_k^\star)\right]. \end{aligned} \tag{1.4.20}$$

Where we took care of the antisymmetric nature of fermion fields with respect to swapping fields by using properties of ϵ:

$$(\chi_N\chi_j) = \chi_N^T\epsilon\chi_j = \left(\chi_N^T\epsilon\chi_j\right)^T = -\chi_j^T\epsilon^T\chi_N = \chi_j^T\epsilon\chi_N = (\chi_j\chi_N). \tag{1.4.21}$$

We can rewrite Eq.(1.4.20) to get a clear view of the mass matrix:

$$\begin{aligned}-\mathcal{L}_{M+D} = \frac{1}{2}\begin{pmatrix}\chi_1\\ \chi_2\\ \chi_3\\ \chi_N\end{pmatrix}^T \epsilon \begin{pmatrix}0 & 0 & 0 & (M_{\mathrm{D}}^\star)_1\\ 0 & 0 & 0 & (M_{\mathrm{D}}^\star)_2\\ 0 & 0 & 0 & (M_{\mathrm{D}}^\star)_3\\ (M_{\mathrm{D}}^\star)_1 & (M_{\mathrm{D}}^\star)_2 & (M_{\mathrm{D}}^\star)_3 & M_{\mathrm{R}}\end{pmatrix}\begin{pmatrix}\chi_1\\ \chi_2\\ \chi_3\\ \chi_N\end{pmatrix}\\ + \frac{1}{2}\begin{pmatrix}\chi_1^\star\\ \chi_2^\star\\ \chi_3^\star\\ \chi_N^\star\end{pmatrix}^T \bar{\epsilon} \begin{pmatrix}0 & 0 & 0 & (M_{\mathrm{D}})_1\\ 0 & 0 & 0 & (M_{\mathrm{D}})_2\\ 0 & 0 & 0 & (M_{\mathrm{D}})_3\\ (M_{\mathrm{D}})_1 & (M_{\mathrm{D}})_2 & (M_{\mathrm{D}})_3 & M_{\mathrm{R}}\end{pmatrix}\begin{pmatrix}\chi_1^\star\\ \chi_2^\star\\ \chi_3^\star\\ \chi_N^\star\end{pmatrix}.\end{aligned} \tag{1.4.22}$$

At this point we reinforce the choice of a Majorana neutrino once again. If we were to add a Dirac particle, the mass matrix would be larger due to the additional independent spinor in a Dirac bi-spinor. Also, we would not be able to reproduce the upcoming seesaw relations, because the bottom right corner of the mass matrix would be zero.

To find masses of the neutrinos we have to diagonalize the mass matrix. With foresight, we can already tell that the mass matrix has rank 2 and that means that only two of the four eigenvalues are non-zero. We also want to get the neutrino mixing matrix and not just the eigenvalues of the mass matrix, to do so we start by defining the Weyl spinors in mass eigenstates:

$$\xi_a = U_{aj}\chi_j + U_{aN}\chi_N. \tag{1.4.23}$$

This way we also get the inverse transformation:

$$\chi_j = U_{aj}^\star \xi_a \text{ and } \chi_N = U_{aN}^\star \xi_a. \tag{1.4.24}$$

Inserting these inverse transformations into Eq.(1.4.20) and requiring the mass terms to be diagonal we get:

$$\begin{aligned}-\mathcal{L}_{M+D} &= \frac{1}{2}\xi_a^T \epsilon \xi_b \left(U_{aN}^\star M_{\mathrm{R}}^\star U_{bN}^\star + U_{aN}^\star (M_{\mathrm{D}}^\star)_k U_{bk}^\star + U_{aj}^\star (M_{\mathrm{D}}^\star)_j U_{bN}^\star\right)\\ &+ \frac{1}{2}\xi_a^\dagger \epsilon \xi_b^\star \left(U_{aN} M_{\mathrm{R}} U_{bN} + U_{aj}(M_{\mathrm{D}})_j U_{bN} + U_{aN}(M_{\mathrm{D}})_k U_{bk}\right)\\ &= \frac{1}{2} m_c^\star \xi_a^T \epsilon \xi_b + \frac{1}{2} m_c \xi_a^\dagger \epsilon \xi_b^\star.\end{aligned} \tag{1.4.25}$$

We also require the masses to be real:

$$m_c^\star = m_c. \tag{1.4.26}$$

From this we get the seesaw condition:

$$U_{aN} M_{\mathrm{R}} U_{bN} + U_{aj}(M_{\mathrm{D}})_j U_{bN} + U_{aN}(M_{\mathrm{D}})_k U_{bk} = m_a \delta_{ab}. \tag{1.4.27}$$

We note that the Dirac mass parameters $(M_{\mathrm{D}})_k$ can be renamed to $(M_{\mathrm{D}})_1 = (M_{\mathrm{D}})_e$, $(M_{\mathrm{D}})_2 = (M_{\mathrm{D}})_\mu$, $(M_{\mathrm{D}})_3 = (M_{\mathrm{D}})_\tau$, since these neutrino flavour states are already defined by charged

fermion mass eigenstates. With this slightly changed notation we can rewrite the seesaw condition in matrix form:

$$\begin{aligned}&\begin{pmatrix} U_{ae} & U_{a\mu} & U_{a\tau} & U_{aN}\end{pmatrix}\begin{pmatrix} 0 & 0 & 0 & (M_{\mathrm{D}})_e \\ 0 & 0 & 0 & (M_{\mathrm{D}})_\mu \\ 0 & 0 & 0 & (M_{\mathrm{D}})_\tau \\ (M_{\mathrm{D}})_e & (M_{\mathrm{D}})_\mu & (M_{\mathrm{D}})_\tau & M_{\mathrm{R}}\end{pmatrix}\begin{pmatrix} U_{be} & U_{b\mu} & U_{b\tau} & U_{bN}\end{pmatrix}^T \\ &= \left[U_{(\nu)}M_{(\nu)}U_{(\nu)}^T\right]_{ab} = \hat{m}_{ab} = \begin{pmatrix} m_1 & 0 & 0 & 0 \\ 0 & m_2 & 0 & 0 \\ 0 & 0 & m_3 & 0 \\ 0 & 0 & 0 & m_4\end{pmatrix} = \begin{pmatrix} 0 & 0 & 0 & 0 \\ 0 & 0 & 0 & 0 \\ 0 & 0 & m_3 & 0 \\ 0 & 0 & 0 & m_4\end{pmatrix}.\end{aligned} \tag{1.4.28}$$

By rewriting Eq.(1.4.28) like $U_{(\nu)}M_{(\nu)} = \hat{m}U_{(\nu)}^\star$ we are able to get conditions for elements of the matrix $U_{(\nu)}$:

$$U_{1N}(M_{\mathrm{D}})_e = U_{1N}(M_{\mathrm{D}})_\mu = U_{1N}(M_{\mathrm{D}})_\tau = U_{2N}(M_{\mathrm{D}})_e = U_{2N}(M_{\mathrm{D}})_\mu = U_{2N}(M_{\mathrm{D}})_\tau = 0, \tag{1.4.29}$$

which tells us that $U_{1N} = U_{2N} = 0$. We also get:

$$U_{1e}(M_{\mathrm{D}})_e + U_{1\mu}(M_{\mathrm{D}})_\mu + U_{1\tau}(M_{\mathrm{D}})_\tau = U_{2e}(M_{\mathrm{D}})_e + U_{2\mu}(M_{\mathrm{D}})_\mu + U_{2\tau}(M_{\mathrm{D}})_\tau = 0 \tag{1.4.30}$$

and this tells us that the vectors U_{1j}, U_{2j} and $((M_{\mathrm{D}})_j, M_{\mathrm{R}})$ are orthogonal. Orthogonality of U_{1j} and U_{2j} follows from the unitarity of $U_{(\nu)}$, since both of these vectors belong to the same eigenvalue of 0.

Because the components of U_{1N} and U_{2N} are equal to 0 and the unitarity of matrix $U_{(\nu)}$ requires $|U_{jN}| = 1$ we can parametrize this vector in the following way:

$$U_{3N} = e^{\mathrm{i}\alpha_3}\sin\theta = \eta_3 s \text{ and } U_{4N} = e^{\mathrm{i}\alpha_4}\cos\theta = \eta_4 c. \tag{1.4.31}$$

With this parametrization we rewrite $U_{(\nu)}M_{(\nu)}$ and get:

$$\begin{pmatrix} U_{1e} & U_{1\mu} & U_{1\tau} & 0 \\ U_{2e} & U_{2\mu} & U_{2\tau} & 0 \\ U_{3e} & U_{3\mu} & U_{3\tau} & \eta_3 s \\ U_{4e} & U_{4\mu} & U_{4\tau} & \eta_4 c\end{pmatrix} M_{(\nu)} = \begin{pmatrix} 0 & 0 & 0 & 0 \\ 0 & 0 & 0 & 0 \\ \eta_3 s(M_{\mathrm{D}})_e & \eta_3 s(M_{\mathrm{D}})_\mu & \eta_3 s(M_{\mathrm{D}})_\tau & (UM)_{34} \\ \eta_4 s(M_{\mathrm{D}})_e & \eta_4 s(M_{\mathrm{D}})_\mu & \eta_4 s(M_{\mathrm{D}})_\tau & (UM)_{44}\end{pmatrix}. \tag{1.4.32}$$

With abbreviations:

$$\begin{aligned}(UM)_{34} &= U_{3e}(M_{\mathrm{D}})_e + U_{3\mu}(M_{\mathrm{D}})_\mu + U_{3\tau}(M_{\mathrm{D}})_\tau + \eta_3 s M_{\mathrm{R}}, \\ (UM)_{44} &= U_{4e}(M_{\mathrm{D}})_e + U_{4\mu}(M_{\mathrm{D}})_\mu + U_{4\tau}(M_{\mathrm{D}})_\tau + \eta_4 c M_{\mathrm{R}}.\end{aligned} \tag{1.4.33}$$

We now solve $\hat{m}U_{(\nu)}$ using Eq.(1.4.32) and get:

$$m_3 U_{3j}^\star = \eta_3 s(M_{\mathrm{D}})_j \text{ and } m_4 U_{4j}^\star = \eta_4 c(M_{\mathrm{D}})_j. \tag{1.4.34}$$

Plugging these relations into abbreviations $(UM)_{34}$ and $(UM)_{44}$ we get:

$$\begin{aligned}(UM)_{34} &= \eta_3^\star s\frac{m_{\mathrm{D}}^2}{m_3} + \eta_3 s M_{\mathrm{R}}, \\ (UM)_{44} &= \eta_3^\star c\frac{m_{\mathrm{D}}^2}{m_4} + \eta_4 c M_{\mathrm{R}}.\end{aligned} \tag{1.4.35}$$

Here we have defined:

$$m_{\mathrm{D}}^2 = |(M_{\mathrm{D}})_e|^2 + |(M_{\mathrm{D}})_\mu|^2 + |(M_{\mathrm{D}})_\tau|^2. \tag{1.4.36}$$

We assume the hierarchy $m_3 \ll m_4 \sim M_{\mathrm{R}}$ with which Eq.(1.4.35) can be solved if $\eta_3^2 = -1$ and $\eta_4^2 = 1$. The masses that we get are:

$$m_{3,4} = \frac{1}{2}\left[\mp M_{\mathrm{R}} + \sqrt{M_{\mathrm{R}}^2 + 4m_{\mathrm{D}}^2}\right] \tag{1.4.37}$$

and produce the usual seesaw relations:

$$m_3 m_4 = \frac{1}{4}\left[-M_{\mathrm{R}}^2 + (M_{\mathrm{R}}^2 + 4m_{\mathrm{D}}^2)\right] = m_{\mathrm{D}}^2 \text{ and } m_4 - m_3 = M_{\mathrm{R}}. \tag{1.4.38}$$

Using the unitarity of $U_{(\nu)}$ as well as the seesaw relations we determine the seesaw angle θ which was introduced in Eq.(1.4.31):

$$\begin{aligned} 1 &= |U_{3e}|^2 + |U_{3\mu}|^2 + |U_{3\tau}|^2 + s^2 = s^2\frac{m_{\mathrm{D}}^2}{m_3^2} + s^2 = s^2\frac{m_4 + m_3}{m_3}, \\ 1 &= |U_{4e}|^2 + |U_{4\mu}|^2 + |U_{4\tau}|^2 + c^2 = c^2\frac{m_{\mathrm{D}}^2}{m_3^2} + c^2 = c^2\frac{m_4 + m_3}{m_4}. \end{aligned} \tag{1.4.39}$$

The solutions are:

$$c^2 = \cos^2\theta = \frac{m_4}{m_4 + m_3} \text{ and } s^2 = \sin^2\theta = \frac{m_3}{m_4 + m_3}. \tag{1.4.40}$$

These solutions allow to rewrite U_{3j} and U_{4j}:

$$U_{3j} = \mathrm{i}c\frac{s}{c}\frac{(M_{\mathrm{D}}^\star)_j}{m_3} = \mathrm{i}c\frac{\sqrt{m_3}}{\sqrt{m_4}}\frac{(M_{\mathrm{D}}^\star)_j}{m_3} = \mathrm{i}c\frac{(M_{\mathrm{D}}^\star)_j}{m_{\mathrm{D}}} \text{ and } U_{4j} = s\frac{(M_{\mathrm{D}}^\star)_j}{m_{\mathrm{D}}}. \tag{1.4.41}$$

We can finally write down our neutrino mixing matrix:

$$U_{(\nu)} = \begin{pmatrix} U_{1e} & U_{1\mu} & U_{1\tau} & 0 \\ U_{2e} & U_{2\mu} & U_{2\tau} & 0 \\ \mathrm{i}c\frac{(M_{\mathrm{D}}^\star)_e}{m_{\mathrm{D}}} & \mathrm{i}c\frac{(M_{\mathrm{D}}^\star)_\mu}{m_{\mathrm{D}}} & \mathrm{i}c\frac{(M_{\mathrm{D}}^\star)_\tau}{m_{\mathrm{D}}} & -\mathrm{i}s \\ s\frac{(M_{\mathrm{D}}^\star)_e}{m_{\mathrm{D}}} & s\frac{(M_{\mathrm{D}}^\star)_\mu}{m_{\mathrm{D}}} & s\frac{(M_{\mathrm{D}}^\star)_\tau}{m_{\mathrm{D}}} & c \end{pmatrix} \approx \begin{pmatrix} U_{1e} & U_{1\mu} & U_{1\tau} & 0 \\ U_{2e} & U_{2\mu} & U_{2\tau} & 0 \\ \mathrm{i}c\frac{(M_{\mathrm{D}}^\star)_e}{m_{\mathrm{D}}} & \mathrm{i}c\frac{(M_{\mathrm{D}}^\star)_\mu}{m_{\mathrm{D}}} & \mathrm{i}c\frac{(M_{\mathrm{D}}^\star)_\tau}{m_{\mathrm{D}}} & 0 \\ 0 & 0 & 0 & 1 \end{pmatrix}. \tag{1.4.42}$$

Here we neglected the terms with sine of θ and approximated the cosine to 1. With this approximation we get a block diagonal matrix, which tells us that the light states do not mix with the Majorana neutrino. The bigger block is also the traditional neutrino mixing matrix - the U_{PMNS} [20, 21] matrix. This 0th order seesaw approximation also relates the Dirac mass term with the third row of the neutrino mixing matrix $U_{(\nu)}$.

Looking back at the diagonalized mass matrix, we restate that we still have two degenerate massless states. We are going to deal with this in the following section where we discuss 1-loop corrections.

1.4.4 1-loop corrections

As briefly mentioned above, we use one loop corrections to generate masses to the yet massless neutrino states. Going into full detail about 1-loop corrections is beyond the scope of this thesis and mostly simple explanations and quotation of results [1] are presented.

In essence, there are two types of Feynman diagrams, tree and loop. In most cases tree level diagrams are the basis, or lowest order, diagrams for a certain process that do not contain any loops, while loop diagrams describe corrections to that process. They are considered to be corrections, because higher powers of coupling constants arise as there are more vertices in Feynman diagrams. In more technical terms, loop diagrams correspond to higher order terms of the series expansion of the path integral. Though, even being called corrections, these terms do not necessarily have contributions smaller than tree level terms.

As a well-known example, vacuum polarization can be mentioned. It is impossible to measure the real electric charge of the electron due to electron positron pairs being created by the propagating photon. The electron-positron pairs are the loops in the photon propagation diagram and screen the real charge of the electron. Loop corrections do not only screen the electron or give a more accurate branching ratio, but can also give corrections to masses. In the case of the Grimus-Neufeld model the base mass is 0 and loop corrections actually generate the mass.

We move on to indicate the mechanism by which the degenerate neutrinos are distinguished in the Grimus-Neufeld model [1]. The key element to this kind of mass generation are the Yukawa couplings. Yukawas allow interactions that couple bosons and fermions. In our model each of the Higgs doublets have their own Yukawas that couple the left handed doublets to right-handed singlets. In fact, after electroweak symmetry breaking charged fermions acquire masses due to these terms. The Yukawa terms that produce the fermionic mass terms are:

$$-\mathcal{L}_{D_1} = \overline{l}^0_j \phi_a Y^{\bar{a}}_{jk} e^0_{\mathrm{R}k} + \overline{l}^0_j \tilde{\phi}_{\bar{a}} \tilde{Y}^a_j N + h.c. \tag{1.4.43}$$

Here j and k are generation indices. We have ignored terms with quarks and the 0 superscript indicates that the fields are not in their mass eigenstates. We also used the definition of an adjoint doublet:

$$\tilde{\phi}_{\bar{a}} = \epsilon \phi^\star_a = \begin{pmatrix} 0 & 1 \\ -1 & 0 \end{pmatrix} \begin{pmatrix} (\phi^+_a)^\star \\ (\phi^0_a)^\star \end{pmatrix} =: \begin{pmatrix} \phi^{0\star}_{\bar{a}} \\ -\phi^-_{\bar{a}} \end{pmatrix}. \tag{1.4.44}$$

Since the Lagrangian is invariant under the Higgs doublet symmetry the Yukawa couplings also have to transform under the same symmetry:

$$\tilde{Y}^a_{jn} \to \tilde{Y}^{a\prime}_{jn} = U^{a\bar{b}} \tilde{Y}^b_{jn} \text{ and } Y^{\bar{a}}_{jn} \to Y^{\bar{a}\prime}_{jn} = Y^{\bar{b}}_{jn} U^{b\bar{a}}. \tag{1.4.45}$$

To fix the Yukawas we explicitly choose the Higgs basis from Sec.1.4.1. After the first Higgs doublet acquires the VEV we get the fermionic mass terms (without quarks once again):

$$-\mathcal{L}_{D_1}|_{H_a \to 0} = -\frac{v}{\sqrt{2}} \left(\bar{e}^0_{\mathrm{L}j} Y^{\bar{1}}_{jk} e^0_{\mathrm{R}k} + \bar{\nu}^0_{\mathrm{L}j} \tilde{Y}^1_j N + h.c. \right). \tag{1.4.46}$$

As we can see, since the second doublet does not acquire a VEV, the Yukawa couplings to the second doublet do not play a role in mass terms. In Eq.(1.4.46) we know we have mass terms,

but the mass matrix is not diagonal at this point and we want to rewrite these terms in mass eigenstates. To do so we decompose the mass matrix of the charged leptons:

$$(M_e)_{jl} := \frac{v}{\sqrt{2}} Y^{\bar{1}}_{jl} = U^{e\mathrm{L}\dagger}_{jk} \mathrm{diag}\left(m_e, m_\mu, m_\tau\right)_k U^{e\mathrm{R}}_{kl} \tag{1.4.47}$$

and redefine the fermion fields:

$$e^0_{\mathrm{L}j} = U^{e\mathrm{L}\dagger}_{jk} e_{\mathrm{L}k} \ , \ e^0_{\mathrm{R}j} = U^{e\mathrm{R}\dagger}_{jk} e_{\mathrm{R}k} \text{ and } \nu^0_{\mathrm{L}j} = U^{e\mathrm{L}\dagger}_{jk} \nu_{\mathrm{L}k}. \tag{1.4.48}$$

Inserting these into relations into Eq.(1.4.46) we get:

$$-\mathcal{L}_{D_1}|_{H_a} = m_{ek} \left(\bar{e}_{\mathrm{L}k} e_{\mathrm{R}k} + \bar{e}_{\mathrm{R}k} e_{\mathrm{L}k}\right) + \left(\frac{v}{\sqrt{2}} \bar{\nu}_{\mathrm{L}m} U^{e\mathrm{L}\dagger}_{mj} \tilde{Y}^1_j N + h.c.\right). \tag{1.4.49}$$

Here m_{ek} is the diagonal charged lepton mass matrix. With these terms we can see how to define the coupling of neutral fermions to the first doublet already with a hint from Eq.(1.4.15):

$$\tilde{Y}^1_j = U^{e\mathrm{L}}_{jk} \frac{\sqrt{2}}{v} (M_\mathrm{D})_k = U^{e\mathrm{L}}_{jk} (Y^{(1)}_N)_k. \tag{1.4.50}$$

At this point we have a very good hint on how to define the Yukawa coupling to neutral fermions of the second Higgs doublet as well:

$$\tilde{Y}^2_j = U^{e\mathrm{L}}_{jk} (Y^{(2)}_N)_k. \tag{1.4.51}$$

Now we are about to parametrize the Yukawa couplings to the neutral fermions, but before that we restate our neutrino mixing matrix for clarity:

$$\begin{aligned} U_{(\nu)} &= \begin{pmatrix} U_{1e} & U_{1\mu} & U_{1\tau} & 0 \\ U_{2e} & U_{2\mu} & U_{2\tau} & 0 \\ \mathrm{i}c\frac{(M^\star_\mathrm{D})_e}{m_\mathrm{D}} & \mathrm{i}c\frac{(M^\star_\mathrm{D})_\mu}{m_\mathrm{D}} & \mathrm{i}c\frac{(M^\star_\mathrm{D})_\tau}{m_\mathrm{D}} & -\mathrm{i}s \\ s\frac{(M^\star_\mathrm{D})_e}{m_\mathrm{D}} & s\frac{(M^\star_\mathrm{D})_\mu}{m_\mathrm{D}} & s\frac{(M^\star_\mathrm{D})_\tau}{m_\mathrm{D}} & c \end{pmatrix} \\ &= \begin{pmatrix} U_{1e} & U_{1\mu} & U_{1\tau} & 0 \\ U_{2e} & U_{2\mu} & U_{2\tau} & 0 \\ \mathrm{i}c\frac{v}{\sqrt{2}}\frac{(Y^{\star(1)}_N)_e}{m_\mathrm{D}} & \mathrm{i}c\frac{v}{\sqrt{2}}\frac{(Y^{\star(1)}_N)_\mu}{m_\mathrm{D}} & \mathrm{i}c\frac{v}{\sqrt{2}}\frac{(Y^{\star(1)}_N)_\tau}{m_\mathrm{D}} & -\mathrm{i}s \\ s\frac{v}{\sqrt{2}}\frac{(Y^{\star(1)}_N)_e}{m_\mathrm{D}} & s\frac{v}{\sqrt{2}}\frac{(Y^{\star(1)}_N)_\mu}{m_\mathrm{D}} & s\frac{v}{\sqrt{2}}\frac{(Y^{\star(1)}_N)_\tau}{m_\mathrm{D}} & c \end{pmatrix}. \end{aligned} \tag{1.4.52}$$

According to the paper by Grimus and Neufeld [1], with one loop corrections only one additional neutrino gets a mass, while the other of the two degenerate neutrinos remains massless. Having that in mind, we choose our first neutrino to remain massless after loop corrections. Since it remains massless the second Higgs doublet should not couple to it and we can write down the equality:

$$U_{1e}(Y^{(2)}_N)_e + U_{1\mu}(Y^{(2)}_N)_\mu + U_{1\tau}(Y^{(2)}_N)_\tau = 0. \tag{1.4.53}$$

Using the unitarity of the neutrino mixing matrix we can express the Yukawa of the second Higgs doublet to neutral fermions as a linear combination of two other orthonormal vectors:

$$(Y^{(2)}_N)_k := dU_{2k} + d' U_{3k}. \tag{1.4.54}$$

Here $0 < d \in \mathbb{R}$ and $d' \in \mathbb{C}$ are free parameters in the Yukawa coupling.

Now we merely quote the results from Grimus and Neufeld[1]: after diagonalizing the matrix contribution from one loop diagrams we get a mass contribution to the second, previously massless, state which is proportional to d^2. Eq.(4.9) in [1]:

$$\hat{M}_\nu^{(1)} = diag(0, |\mu| d^2, m_3, m_4). \tag{1.4.55}$$

Here μ is a function describing the loop contribution. We see, that we were able to break the degeneracy of the two massless states by generating mass for one of the neutrinos by 1-loop corrections.

1.4.5 Recap of the model

Before discussing parameters of the model we do a brief recap and mention the main ideas. The Grimus-Neufeld model has a heavy Majorana neutrino and two Higgs doublets. Together with the Majorana neutrino a Majorana mass term is added to the Lagrangian. This heavy neutrino couples to a superposition of SM neutrinos with the help of Yukawa couplings from the Higgs doublets. Only one of the Higgs doublets gets a VEV and generates masses at tree level. Rewriting the Majorana mass term together with the Dirac mass terms that couple the light neutrinos with the heavy Majorana neutrino we get the non-diagonal mass matrix. By diagonalizing the matrix we get two massless and two massive states via the seesaw mechanism. At this point the second Higgs doublet and its Yukawa couplings come into play. Loop corrections are proportional to Yukawa couplings and if the Yukawas of first and second doublet are not aligned we are able to generate mass for one of the massless neutrinos.

1.4.6 Theoretical and physical parameters in the model

In order to compare the results of packages we want to do parameter scans, therefore in this section the parameters are introduced. First of all, we want to make a distinction between theoretical and physical parameters. Theoretical parameters are in essence parameters of the Lagrangian, for example, Yukawa couplings, mass parameters and parameters of the Higgs potential. On the other hand, physical parameters are such as masses of observed particles. Software packages take theoretical parameters as input and expressions relating physical and theoretical parameters are needed to do scans over physical parameters. We do have such expressions at tree level for the Higgs sector and at 1-loop level for neutrinos from private discussion with the supervisor [22]. Since showing all of the derivations is simply too much, we only list the parameters and make a few comments concerning the steps taken to arrive at the expressions.

We begin by listing the theoretical part, which at this point should be more or less clear:

- Yukawa couplings to neutrinos
- All the Z_{abcd} parameters of the Higgs potential, that are reduced to 7 parameters in the real case and to 10 in the complex case instead of 16

- The Y_{22} parameter in the Higgs potential, which is denoted as `M222` in the code because it is the mass parameter squared
- Majorana mass parameter
- Yukawa couplings to quarks
- Phase of the second Higgs doublet

We note that not all of the Lagrangian parameters have been listed, since they are related via tadpole equations, which are given by the minimum condition in Eq.(1.2.2). Tadpole equations at tree level give these relations:

$$Y_{11} = -\frac{v^2 Z_{1111}}{2} \tag{1.4.56}$$

and

$$Y_{12} = -\frac{v^2 Z_{1112}}{2}. \tag{1.4.57}$$

Yukawa couplings to leptons, the vacuum expectation value and coupling constants are missing from the parameter list, since they are fixed by the matching to the Standard Model. In addition to the parameters that we do not put in, we also have parameters that are not interesting at the moment. Since in the Grimus-Neufeld model we are mainly interested in the masses of neutrinos we do not scan over Yukawa couplings to quarks and leave them constant. Also, since the phase of the second Higgs doublet is not physical we simply set it to 0, which simplifies expressions and calculations.

We now also list the physical parameters:

- Neutrino data [23]: mass squared differences and the measured PMNS matrix
- Masses of yet unobserved Higgses: m_{H}, m_{A} and $m_{\mathrm{H}^\pm}$
- Fixed mass of the observed Higgs m_{h}
- Mixing angle θ_{12} between the lightest and heavier scalar Higgses and the mixing angle θ_{13} between the light scalar and pseudo scalar Higgses

In our case normal mass hierarchy is assumed and we also have one massless neutrino because only 1-loop corrections are used, therefore mass differences squared give masses of the 2 heavier neutrinos:

$$\tilde{m}_2 = \sqrt{\Delta m^2_{\mathrm{atm}}} \text{ and } \tilde{m}_3 = \sqrt{\Delta m^2_{\mathrm{atm}} + \Delta m^2_{\mathrm{sol}}}. \tag{1.4.58}$$

Here tildes indicate that these are loop corrected and not tree level masses, $\Delta m^2_{\mathrm{atm}}$ and $\Delta m^2_{\mathrm{sol}}$ correspond to atmospheric and solar neutrino data. The masses that we get for the neutrinos are as follows:

$$\begin{aligned} \tilde{m}_2 &= 8.695 \times 10^{-12}\ \mathrm{GeV} \\ \tilde{m}_3 &= 5.124 \times 10^{-11}\ \mathrm{GeV}. \end{aligned} \tag{1.4.59}$$

For the PMNS matrix we set the possible phase to 0 due to large uncertainties.

To relate Higgs masses to the Higgs potential we have tree level relations that come from diagonalizing the Higgs mass matrix. In order to leave the possibility to have mixing of the pseudo scalar Higgs A to the lightest Higgs we allow the parameters to be complex, which means that we have three additional parameters coming from the imaginary parts. Because of this choice we have a few unconstrained parameters since the Higgs mass matrix provides a limited number of relations. The known relations are as follows:

$$Z_{1111} = \frac{c_{12}^2 c_{13}^2 m_{\mathrm{h}}^2 + s_{12}^2 c_{13}^2 m_{\mathrm{H}}^2 + s_{13}^2 m_{\mathrm{A}}^2}{v^2}, \tag{1.4.60}$$

$$Z_{2112} = \frac{c_{12}^2 c_{13}^2 m_{\mathrm{h}}^2 + s_{12}^2 c_{13}^2 m_{\mathrm{H}}^2 + s_{12}^2 \left(m_{\mathrm{h}}^2 + s_{13}^2 m_{\mathrm{H}}^2\right) + c_{13}^2 m_{\mathrm{A}}^2 - 2m_{\mathrm{H}^\pm}}{v^2}, \tag{1.4.61}$$

$$\mathrm{Re}(Z_{2121}) = \frac{c_{12}^2 \left(-s_{13}^2 m_{\mathrm{h}}^2 + m_{\mathrm{H}}^2\right) + s_{12}^2 \left(m_{\mathrm{h}}^2 - s_{13}^2 m_{\mathrm{H}}^2\right) - c_{13}^2 m_{\mathrm{A}}^2}{v^2}, \tag{1.4.62}$$

$$\mathrm{Im}(Z_{2121}) = \frac{2c_{12}s_{12}s_{13}\left(-m_{\mathrm{h}}^2 + m_{\mathrm{H}}^2\right)}{v^2}, \tag{1.4.63}$$

$$\mathrm{Re}(Z_{1112}) = \frac{c_{12}c_{13}s_{12}\left(m_{\mathrm{h}}^2 - m_{\mathrm{H}}^2\right)}{v^2}, \tag{1.4.64}$$

$$\mathrm{Im}(Z_{1112}) = \frac{c_{13}s_{13}\left(-c_{12}^2 m_{\mathrm{h}}^2 - s_{12}^2 m_{\mathrm{H}}^2 + m_{\mathrm{A}}^2\right)}{v^2}. \tag{1.4.65}$$

Here c_{12} and s_{12} are shorthand notations for $\cos(\theta_{12})$ and $\sin(\theta_{12})$. Analogically we have the same notation for the pseudo scalar Higgs A and lightest Higgs h mixing angle θ_{13}. At all times θ_{13} is set to 0 and we immediately see that the imaginary parts become equal to 0. These parameters are plotted in Fig. 1 for a specific set of masses as a dependence on the mixing angle θ_{12}. The unconstrained parameters are: Z_{2222}, Z_{2211}, Z_{2212}, real and imaginary parts of Z_{2212}.

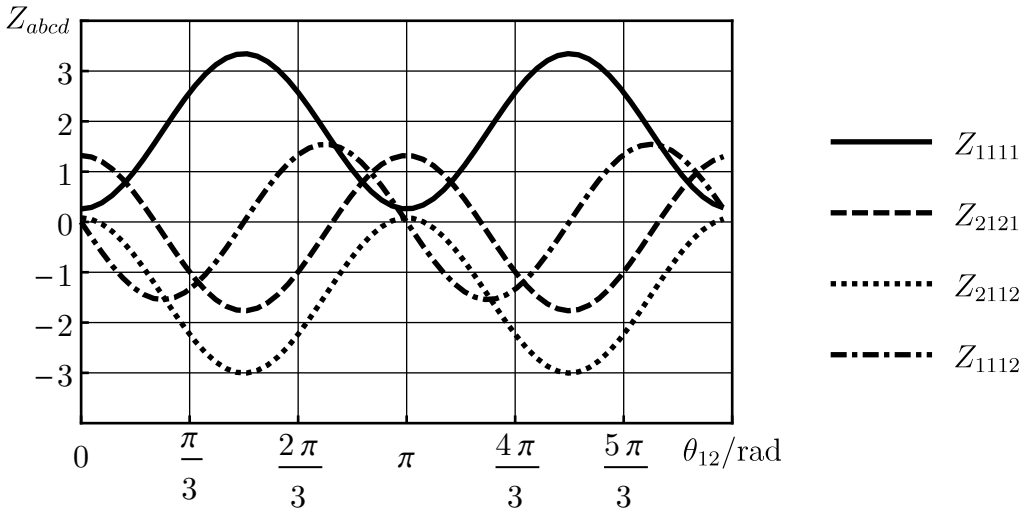

Figure 1. Dependence of known quartic couplings Z_{abcd} on the mixing angle θ_{12} with $m_{\mathrm{h}} = 125.09$ GeV, $m_{\mathrm{H}} = 450$ GeV, $m_{\mathrm{A}} = 350$ GeV, $m_{\mathrm{H}^\pm} = 400$ GeV, and $v = 246$ GeV

The mass matrix of the Higgses provides not only some of the quartic couplings, but also

the Y_{22}, or M_{222}, parameter:

$$M_{222} = m^2_{\mathrm{H}^\pm} - \frac{v^2 Z_{2211}}{2}. \tag{1.4.66}$$

For the neutrino sector the PMNS matrix and mass differences have to transform into the Yukawa couplings to the Higgs doublets. Already in Sec.(1.4.4) we saw that the Yukawa coupling to the first Higgs doublet is related to Dirac mass parameters and the Yukawa coupling to the second Higgs doublet is parametrized with the help of d and d'. Yet, it is not so simple as the parametrization is done at 1-loop level, these parameters depend on the Higgs sector as well as on the neutrino sector and in turn they become huge functions of masses and mixing angles. During calculations d' is parametrized as:

$$d' = |d'| \exp\left[\mathrm{i}\phi\right]. \tag{1.4.67}$$

The absolute value of d' not only depends on the phase ϕ, but also involves dealing with a fourth order polynomial during every calculation. The polynomial has 4 solutions, which we have to filter since $|d'|$ has to be real, positive and we also limit it to be < 1. d is a bit more simple and has a defined expression:

$$d^2 = \frac{v^2 \tilde{m}_2 \tilde{m}_3}{m^2_{\mathrm{D}} |f_1 f_3 + f_2^2|}. \tag{1.4.68}$$

Here f_1, f_2 and f_3 are functions depending on physical input, tildes over masses of the neutrinos denote that these are the measured masses. m^2_{D} comes from Eq.(1.4.38), but since this is no longer tree level we have an additional parameter λ_{D} to account for that:

$$m^2_{\mathrm{D}} \to m^2_{\mathrm{D}} = \lambda_{\mathrm{D}} \tilde{m}_3 \tilde{m}_4. \tag{1.4.69}$$

In essence m^2_{D} is a free parameter, but it should be similar to the tree level relation and therefore we limit λ_{D} to range $0.5 < \lambda_{\mathrm{D}} < 1.5$.

One other change that arises due to an additional massive neutrino after loop corrections is the relation of the neutrino mixing matrix to the measured PMNS matrix:

$$U^\dagger_{ab} = V^{\mathrm{PMNS}}_{ab} \to U = \left(V^{\mathrm{PMNS}} R^T\right)^\dagger. \tag{1.4.70}$$

Here R is the matrix used to rotate the tree level mass eigenstates into the new and loop corrected mass eigenstates. R does not affect the massless and heaviest states. This rotation matrix is parametrized by one angle and three phases and their expressions in terms of physical parameters become quite complicated. Since writing out huge equations will not give much of insight, we only mention that some of the values cannot be uniquely determined and can differ by a sign. On the other hand, quite often parameters get squared and the non-uniqueness with respect to the sign can be fairly safely ignored.

This concludes our discussion of the Grimus-Neufeld model.

1.5 Software

In this final introductory section we mention the more general background of software used in particle physics and specify the packages that we have used in the thesis.

We begin by stating their purpose: software is phenomenology (mostly LHC phenomenology) oriented and is created to speed up the process of calculating observables. In principle, there are quite a few steps before it is possible to have detector specific output. It all starts with the theoretical description and analytical expressions, then using spectrum generators numerical values of masses, branching ratios and specific observables are calculated. Further, using event generators (`Pythia`, `Herwig`) collisions are generated and only then detector simulation (`GEANT`) is done. In this work only the first two steps, i.e. before event generation, are considered and only the first two types of software are used.

For the analytical part (given the particle content, Lagrangian and mixings) `SARAH-4.13.0` [24, 25, 26, 27] provides expressions for mass matrices, tadpole equations, interaction vertices, renormalization group equations, some of loop corrections, etc. These are further employed by the two spectrum generators that we have used. Since the model was fully implemented in `SARAH` during the coursework [2] it will not be of much concern through the remaining part of this paper, except for the parts where we remind about the need to have two slightly different model files for the two spectrum generators.

The spectrum generators that we are using are `SPheno-4.0.3` [7, 8] and `FlexibleSUSY-2.1.0` [3, 4, 5, 6]. Both of them rely on analytical expressions from `SARAH` and the `SPheno` code is even generated by `SARAH`. `FlexibleSUSY` is a `C++` and `Mathematica` framework, while `SPheno` is written in `Fortran`. As mentioned above, the spectrum generators calculate the mass spectrum, branching ratios, physical observables as well as mixing matrices. Using these generators it is not only possible to check parameter points one by one, but also to do parameter scans over a range, though that can require additional effort. In this work using two spectrum generators has two purposes: first of all, we want to compare them as the name of the thesis suggests and secondly, they should more or less match if the model is implemented correctly in both of them and that works as a safety measure.

With this we conclude our introduction and move on to the next section, where we describe the problems, that occurred when implementing the model in `FlexibleSUSY` and `SPheno`.

2 Implementation of the model

In this section we describe how we have finished the implementation of the model and we describe how parameter scans are done with each software package, which also required an additional step of implementation.

Before discussing the spectrum generators we note that we did refine the implementation in SARAH, but did not change the previously described parts. The changes were made to the particles.m and parameters.m files. Since these files were based on stock model files, which had a couple of slight mistakes, we fixed them just to be sure that everything is correct. Fixes included giving or correcting names to particles and parameters, defining parameter SLHA (SUSY Les Houches Accord) [28] blocks, changing where and how certain particles were described. In the main model file we have also defined the spinors in the high energy regime. Though, that is a relic coming from older SARAH versions and is supposedly not used any more. SARAH's CheckModel[] command and the SARAH Forum [29] guided the process.

2.1 Implementation in FlexibleSUSY

We begin by describing FlexibleSUSY since this is the package that failed to run previously: it either did not compile at all or would not perform calculations. Before we thought that the explicit 0 VEV causes problems, but that turned out to be not the case. Problems were caused by tadpole equations, a small bug in the package and the interplay with SARAH definitions. In addition, the way complex parameters are described in the FlexibleSUSY model file also caused a bit of trouble when describing complex parameters.

We start with the more simple part of complex parameters. As long as parameters are defined as complex in SARAH no additional steps are required in SPheno, but FlexibleSUSY requires to define the real and imaginary parts separately. In addition, it is important to add the line in FlexibleSUSY model file:

```
RealParameters={};
```

Code 1. Definition of real parameters

Without this line all of the parameters are treated as real, since that is the default. When no parameters are given, definitions from SARAH are used. To have the imaginary parts included it is needed to define the real and complex part separately. For example, the definition of Yukawa coupling to the first Higgs doublet looks like this:

```
FSAuxiliaryParameterInfo={
       {Yv1rIN, { InputParameter->True,
                  ParameterDimensions-> {3},
                  LesHouches -> YV1IN
                } },
       {Yv1iIN, { InputParameter->True,
                  ParameterDimensions-> {3},
```

```
                  LesHouches -> IMYV1IN
                } }
        <...>
}
```

Code 2. Defining real and imaginary parts of complex input parameters

Hereinafter <. . .> indicates skipped lines. The definition is more or less obvious, it is needed to specify whether the parameter is an input parameter, parameter's dimensions (scalar, vector and etc.) and the corresponding Les Houches input block. Later on these definitions are supplied to the original input parameter:

```
LowScaleInput = {
   {v, LowEnergyConstant[vev]},
        <...>
   {Yv1, Yv1rIN+I*Yv1iIN},
        <...>
};
```

Code 3. Connecting real and imaginary parts to the input parameter

Here `I` stands for the imaginary unit.

In the case of the more complicated problem of tadpole equations the problem hid in numerically ill-defined solutions to the equations. The tadpole equations get a bit complicated due to the included phase of the second Higgs doublet and the default solution method is not sufficient. Even though the solutions are analytically correct, when numerical calculations are done for the phase of 0 division by 0 occurs and that in turn stops the calculation. To overcome this, alternative solutions have to be provided in the `FlexibleSUSY` model file [30]:

```
TreeLevelEWSBSolution = List @@@ {
        M112 -> -((v^3 Z1111 - tadpole[1])/v),
        Re[M12] -> (1/(4 v)) E^(-I eta) (-E^(I eta) v^3 Z1112 -
                        E^(I eta) v^3 conj[Z1112] +
                        2 tadpole[2] + 2 E^(2 I eta) tadpole[2] - 2 I tadpole[3] +
                        2 I E^(2 I eta) tadpole[3]),
        Im[M12] -> -(1/(4 v)) E^(-I eta) (-I E^(I eta) v^3 Z1112 +
                        I E^(I eta) v^3 conj[Z1112] + 2 I tadpole[2] -
                        2 I E^(2 I eta) tadpole[2] +
                        2 tadpole[3] + 2 E^(2 I eta) tadpole[3])
};
```

Code 4. Alternative solutions to the tadpole equations

Here we can see that the solutions are given for the parameters M_{112} and M_{12}. These solutions behave normally and do not cause problems. Though, they do look more complicated than in Eq.(1.4.56) and Eq.(1.4.57) due to the phase η (`eta`) not yet set to 0, not separating the real and

imaginary parts of parameters as well as for having the `tadpole[i]`, which are internally used by `FlexibleSUSY`.

At this part also emerges a small error, or a *bug*, in the software package. When solving the tadpole equations for complex parameters it is needed to specify to solve for the real and imaginary parts separately. This caused a duplicate line in the code generated by `FlexibleSUSY`, which caused compilation failures. Of course, it is quite hard to identify that an error is caused by a bug in the package and a lot of time was spent trying to overcome this compilation failure by refining the model file. Eventually, we contacted dr. A.Voigt and dr. P.Athron, who are the co-developers of the package, for guidance [30]. They did help with both problems related to the tadpole equations and a few other questions that we had. The bug with duplicate lines was in the version `2.0.1` and is fixed in the new `2.1.0` release.

With these issues, that took a huge amount of time, cleared `FlexibleSUSY` is now fully functioning. We now move on to describe the scanning of parameters.

2.1.1 `Mathematica` interface

In this part we introduce the scanning interface, how the physical parameters are transformed into theoretical and are passed to the package.

Fortunately, in addition to the `terminal` based interface `FlexibleSUSY` also provides a `Mathematica` interface, which makes everything a lot easier and performing simple scans is not a problem. In essence, there are two steps needed to do a scan: 1) defining a function to put in specified parameters, 2) using `Mathematica`'s built-in tools to generate parameter ranges, save, and plot the output.

For the first step the general structure of the scanning function is quite straightforward and is written out in Code 5. The `Mathematica`'s `Module[local,expression]` environment comes in handy, since it is possible to localize the calculation. Inside the `Module` we first do the necessary calculations and transform the parameters, then the `FlexibleSUSY` interface is called. A calculation specific `handle` is opened, which consists of `fsSettings`, `fsSMParameters`, and `ModelParameters`. In `fsSettings` settings are passed to the package by giving values for various flags, such as inclusion of 2-loop Higgs mass corrections, calculation precision, forcing positive masses and etc. We will specify the used flags in sections concerning the actual scanning. In `SMParameters`, as the name suggests, Standard Model-specific parameters, such as the Higgs mass, masses of electron, muon and tau, are passed down. In `ModelParameters` the theoretical parameters of the model are passed and this is where our input goes in. In all three parts the passing down is done via `Mathematica`'s replacement rules. After specifying the `handle` the `spectrum` is calculated and the `handle` is closed. Further, the `If[]` statement checks whether the calculation succeeded or not and gives appropriate output. In this example the model name is `Flexible312` and the `spectrum` is given as the replacement rule for the model name. After the replacement the model name becomes a list of other replacement rules, that now have the values of various output parameters. Using the `Mathematica`-specific syntax this example outputs a multiplet (list) of Higgs masses `Pole[M[hh]]`.

```
ScanOver[<input_parameters>] :=
    Module[{<local>},
        <Precalculations_and_passing_input>
        handle = FSFlexible312OpenHandle[
                fsSettings -> {Setting->Value,
                                <...>},
                fsSMParameters -> {SMparameter->Value,
                                <...>},
                fsModelParameters -> {ModelParameter->Value,
                                <...>}
                ];
        spectrum = FSFlexible312CalculateSpectrum[handle];
        FSFlexible312CloseHandle[handle];
        If[spectrum === $Failed,
              Array[invalid&, 1],
              Pole[M[hh]]/.(Flexible312 /. spectrum)
              ]
    ]
```

Code 5. General layout of the scanning function

For the second part we use the tools provided by `Mathematica` and layout the general structure in Code 6. At first we generate a range of values for a certain parameter, then we launch multiple kernels in order to use parallel computing and save some time. In the `ParallelTable[expression, range]` we scan over the range and as output we get a list of lists, which is a `Mathematica` structure, containing the input parameter from the range and outputs of the `ScanOver[]`. We can also have n-dimensional parameter scans over multiple ranges and have the `ScanOver[]` function take in more arguments. Though, doing n-dimensional scans takes a lot more time and does not necessarily give additional insight. Additionally, we monitor the overall progress of the scan, but this is not implemented in the example. Later on we delete invalid outputs and export the data into a text file for later access. That concludes the implementation in `FlexibleSUSY` and we move on to to discuss `SPheno`.

```
range=Range[start, end, step];
LaunchKernels[];
DistributeDefinitions[ScanOver];
data=ParallelTable[
        {range[[k]],ScanOver[ range[[k]] ]},{k, Length[range]}
];
```

Code 6. Structure of performing the scan

2.2 Implementation in SPheno

Even though SPheno was said to be fully working in the course work, in this section we return to make a few remarks and introduce changes.

First of all, it would be ideal to have the same SARAH model file for SPheno and FlexibleSUSY where we have the vacuum expectation value of the second Higgs doublet set to 0 explicitly. Yet, after consulting with dr. F.Staub [31], the developer of SARAH and co-developer of SPheno, we got the answer that this is impossible for our model and we continue to use the previous approach, where we have a temporary vacuum expectation value.

One change that we had to make in the model file is related to the masses of neutrinos. Double precision (64 bit) is not enough, when it is needed to calculate the masses of neutrinos. This is related to the discussion about mass matrices in Sec.(1.2). Though, double precision is enough in case of real parameters since then it is enough to diagonalize M instead of $M^\dagger M$. To have quadruple precision (128 bit) enabled a few alterations have to be made. First of all, in the SPheno model file we have to specify for which particles quadruple precision will be used:

```
QuadruplePrecision = {Fv};
```

Code 7. Quadruple precision in the SPheno model file

Here the neutrinos are called Fv and we enable quadruple precision for them. To really have quadruple precision enabled it is also needed to edit the Makefile in SPheno's src directory and recompile everything. The edit is quite simple, it is only needed to remove the -DONLYDOUBLE flag as shown below:

```
# PreDef = -DGENERATIONMIXING -DSEESAWIII -DONLYDOUBLE
PreDef = -DGENERATIONMIXING -DSEESAWIII
```

Code 8. Quadruple precision in the Makefile

Here the commented line starts with #.

Unfortunately, due to the approach that SPheno uses to diagonalize complex symmetric matrices in order to get real and positive eigenvalues, even quadruple precision falls short for neutrino masses. With quadruple precision in SPheno, according to F.Staub, approximately 30 digits come out correctly. Now, in the neutrino mass matrix we have the mass $M_{\rm R}$ of a Majorana neutrino, which is heavy and starts at order of hundreds of GeV, and the previously mentioned light neutrinos, for which we expect masses on the order of $10^{-10} - 10^{-12}$ GeV. Due to the limited amount of significant digits, we cannot have the ratio of the squared masses of light neutrinos to the heavy neutrino smaller than $\approx 10^{-30}$, or, in other words, $M_{\rm R}$ can be up to $\approx 10^3$. So far, everything would be fine, but after some investigation, we have found that in the process SPheno computes eigenvalues to the fourth power and the available light neutrino masses are limited to the minimum of $10^{-6} - 10^{-5}$ GeV. As to why exactly SPheno computes fourth order eigenvalues would require further investigation, which is not in the range of the thesis. The conclusion is that at this moment SPheno is not sufficient in the neutrino sector, which is the most important part of the Grimus-Neufeld model.

However, FlexibleSUSY uses a different approach in dealing with the masses of neutrinos, or with complex symmetric matrices in general. Despite the fact that double precision is used, it is possible to calculate the masses of the neutrinos. FlexibleSUSY uses Takagi's factorization, which is implemented via [32]. In essence, by using this type of factorization it is possible to diagonalize the mass matrix and get square roots of $M^\dagger M$ eigenvalues without actually having $M^\dagger M$ matrix and that avoids having higher orders of powers for the masses.

2.2.1 Scanning and the SSS package

In this part we discuss the way scanning is done with SPheno and how it was implemented.

First of all, we note that SPheno does not have a native Mathematica interface like FlexibleSUSY, but on the other hand there is a special Mathematica package SSP-1.2.5[33] for doing scans. However, even being a Mathematica package SSP is not able to use all of the tools provided by Mathematica and that greatly complicated all of the needed precalculation. In fact, due to the specific way the scanning parameters are entered, SSP cannot use any of the functions like If[], Solve[], etc. In other words, it became impossible to deal with the fourth order polynomial required for d'. To overcome this we have made our own scanning tool, which is called the SSS, or Simono SPheno Scan. In making the package we had two goals in mind: 1) to be able to use Mathematica's built-in fucnctionality and 2) to have the scanning process as similar to FlexibleSUSY as possible. It also turns out that the package can be easily adapted to any other SPheno model by simply defining new parameters. We have succeeded in our goals and here we describe the working principle and main elements of the package as well as mention a couple of differences as compared to FlexibleSUSY.

The idea behind the operation of the package is to take in a list of replacements, write an appropriate input file, call SPheno, read the output file and eventually return a list of required values. The package consists of three files: Cutter, SPhenoParams.m and SSS.m. Cutter is a little bash script that cuts away the unnecessary blocks of the output file in order to make it shorter and therefore shrink the amount of data the package has to go through when searching for specific blocks. In SPhenoParams.m, as the name suggests, we have the names for flags and parameters defined, as well as default values and some permanent values, for example, the Standard Model parameters. For a quick glance we show the general structure of defining the names:

```
ParamBlocks:={
{"Block␣NAME",{
          {Parameter_Number,Parameter_Name},
          <...> },
<...> }
```

Code 9. Structure used in SPhenoParams.m

␣ simply denotes a space. Here one entry in the ParamBlocks is a list that contains the name of the block as the first entry and the second entry contains a list of parameter names, which are

numbered according to SLHA conventions and definitions in the SPheno model file. It is worth to mention, that for defining matrices and vectors we use a slightly different approach:

```
ParamBlocks:={
<...>
{"Block␣MATRIX", Table[{n,m,Matrix[[n,m]]},{n,3},{m,3}]
          }
<...> }
```

Code 10. Matrix entries in SPhenoParams.m

Here we have the Table[] generating necessary entries, in this example entries for the 3×3 matrix Matrix. In this way we save some time in writing all of the entries one by one, though at every start of a scan there is a warning message which informs that Mathematica does not know the size of Matrix. Despite that the package functions as intended. As mentioned, SPhenoParams.m also has a list of default values, which are simply implemented as:

```
DefReps={
Parameter_Name->Value,
<...> }
```

Code 11. Default values SPhenoParams.m

The SSS.m file contains all the functions: WriteLH, ReadLH, Saver and GetSpectrum. The first function writes an input file, the next one reads an output file. Saver is used to cut down the produced data even more. It takes in a list of block names that are to be saved, while discarding everything else. Finally, GetSpectrum uses the writing and reading functions to call SPheno and acquire the output. The GetSpectrum takes in the paths to SPheno executable, input and output files and a list of replacement rules that are later passed down to writing and reading functions. This part is written in a general way and is independent of changes made to SPhenoParams.m. Just like FlexibleSUSY's handle is opened for a single calculation, GetSpectrum is also called for each calculation separately.

As noted above, we have succeeded in making the usage of SSS.m similar to that of FlexibleSUSY and that is shown in Code 12. We can see that the implementation is very much like in the case of FlexibleSUSY. The difference being that we do not have to open handles and pass down the theoretical parameters together with the flags for settings in a single list of replacement rules. If some of the parameters are not in the list, default values are used, which can also be easily edited. We also clearly see how GetSpectrum and Saver are used to get the final output. We note that in the real case we do have some safety measures in case of bad parameter points or non-existence of solutions to the absolute value of d'. In the latter case we skip the calculation entirely and write invalid as output.

```
KeepEntries={<blocks_to_be_kept>};
ScanOver[<input_parameters>]:=
  Module[{<local_variables>},
              <precalculations>
```

```
            replace={
                    <setting_flag>->Value,
                    <parameter_name>->Value,
                    <...>
            }
            out=GetSpectrum[<SPheno_dir>,<input_file_dir>,
                            <output_file_dir>,replace];
            out=Saver[out,KeepEntries]
]
```

Code 12. Usage of the `SSS.m` package

The part where the scanning is performed differs from `FlexibleSUSY` only by not using parallel computing. It was not implemented due to the limited amount of time.

With this we finish the part of implementation and move on to discuss the performed scans and how `FlexibleSUSY` compares to `SPheno`.

3 Scans and comparisons

In this final section we compare FlexibleSUSY and SPheno in the Grimus-Neufeld model. This section is divided into two main parts: the Higgs and neutrino sectors.

We note that constant and relevant settings used by both packages during scanning can be found in Appendix A.

3.1 Higgs sector

We first start by doing comparisons in the Higgs sector by setting the Yukawa couplings to neutrinos to zero. Since we do have tree level relations, we try to get back our input from the packages at tree level. Next, we see how much the loop corrections alter our results and how the packages compare.

3.1.1 Tree-level

In this part we do parameter scans at tree level, meaning that the loop corrections to masses are turned off. The flags relevant to loop corrections and their values are listed below. The LesHouches column denotes the number of the flag in the specified block, in SLHA input format.

Table 3. Flags in Block FlexibleSUSY at tree level

LesHouches	Mathematica name	Value
4	poleMassLoopOrder	0
5	ewsbLoopOrder	0

Table 4. Flag in Block SPhenoInput at tree level

LesHouches	Mathematica name	Value
55	LoopMass	0

The flags poleMassLoopOrder and ewsbLoopOrder in FlexibleSUSY correspond to LoopMass in SPheno and control the order of loop corrections applied to masses.

Before beginning the comparison of packages, we note that we had to slightly alter the parameters of the Higgs potential described in Sec. 1.4.6. The change comes from trying to pin down parameter ranges where the mass of the lightest Higgs boson is closest to the measured mass. We did this by matching the inputs and outputs to the Inert Two Higgs Doublet Model (iTHDM) provided in the stock SARAH model files, since it is also written in the Higgs basis.

We have compiled iTHDM and taken a look at the default working point. We tested that point in iTHDM as well as in the Higgs potential in our model and got out only slightly differing masses. The important thing is that the mass of the lightest Higgs boson was around 125 GeV.

We then inserted the masses that we got out from the default working point into our expressions for the Z_{abcd} parameters and the masses that we got out were different from what was expected. After comparing the default iTHDM working point and the calculated parameters it was clear that two of them needed a little tweak. The changes are as follows:

$$Z_{1111} \to \frac{Z_{1111}}{2} \tag{3.1.1}$$

and

$$Z_{2121} \to -\frac{Z_{2121}}{2}. \tag{3.1.2}$$

We see that these alterations are not essential and are merely a matter of used conventions. With the newly defined inputs we were able to get back the masses that we have put in. At this point we also note that since we do not have relations for all the parameters of the Higgs potential we borrow some from the iTHDM while setting the unknown parameter to 0:

$$Z_{2222} = 0.27, \tag{3.1.3}$$

$$Z_{2211} = 1, \tag{3.1.4}$$

$$\mathrm{Re}(Z_{2212}) = \mathrm{Im}(Z_{2212}) = 0. \tag{3.1.5}$$

We note that iTHDM was compiled with `SPheno` and for the Higgs potential in the Grimus-Neufeld model we mainly looked at `FlexibleSUSY`.

With the altered parameters we scan over the mass m_{H} of the heavier scalar Higgs H and the results can be seen in Fig. 2. The parameter point is further specified in the caption of the figure, though we notice that the selected range of $m_{\mathrm{H}}^{\mathrm{in}}$ starts at $m_{\mathrm{A}}^{\mathrm{in}}$ and is according to the constraints specified in [34]. Mass of the charged Higgs is chosen to be larger than the highest excluded mass in Particle Data Group review [17]. Mass of the pseudo scalar Higgs is chosen to be similar to the mass used in the analysis of d' by [35], which is also higher than the excluded masses in PDG review.

In Fig. 2 it is immediately seen that we are able to get back the input at tree level from both packages. The masses stay constant for h, A and $H^{\pm}$ over the whole range of $m_{\mathrm{H}}^{\mathrm{in}}$ and $m_{\mathrm{H}}^{\mathrm{out}}$ nicely follows the line $m_{\mathrm{H}}^{\mathrm{in}} = m_{\mathrm{H}}^{\mathrm{out}}$. Yet, while `FlexibleSUSY` returns input masses precisely, `SPheno` shows small deviations of up to 0.24 %, that amount to a difference of 0.3 GeV. These differences are not visible in the plot of $m_{\mathrm{H}}^{\mathrm{out}}$ due to the scale. At this point we also note, that it was indeed useful to have two software packages, because at first we had differences of over 20 GeV for the mass of h. This eventually lead to finding typos in the `SSS` package when writing down the Standard Model parameters. Now the required SM parameters are matched for both packages and can be found in Appendix A, Table 12. Previously, the typos introduced incorrectly calculated vacuum expectation value, which differed from the one used in the calculation of the Higgs potential parameters and the one used in `FlexibleSUSY`. For calculations of the Higgs potential parameters we use the same VEV as in `FlexibleSUSY`

$$v_{\mathrm{SM}} = 246.22 \text{ GeV} \tag{3.1.6}$$

which also matches the numerical value of [36]

$$v_{\mathrm{SM}} = \sqrt{\frac{1}{\sqrt{2}G_{\mathrm{F}}^{0}}} \approx 246.22 \text{ GeV} \tag{3.1.7}$$

with the value of reduced Fermi's constant from Table 12. The v_{SM} used in `SPheno` is probably still a little different as there is more than one way to calculate the VEV and the used values bring in numerical inaccuracies. The used expressions can be found in [4], Eq. (35) for `FlexibleSUSY` and in [37], Eq. (A.15) for `SPheno`. After trying different VEVs for `SPheno`, the difference was drastically shrunk which proves that the numerical differences in VEVs are the source of this inconsistency. The plot with a different VEV for `SPheno` can be found in Appendix B, Fig. 10. In the following scans we have kept the $v_{\mathrm{SM}} = 246.22$ GeV for both packages.

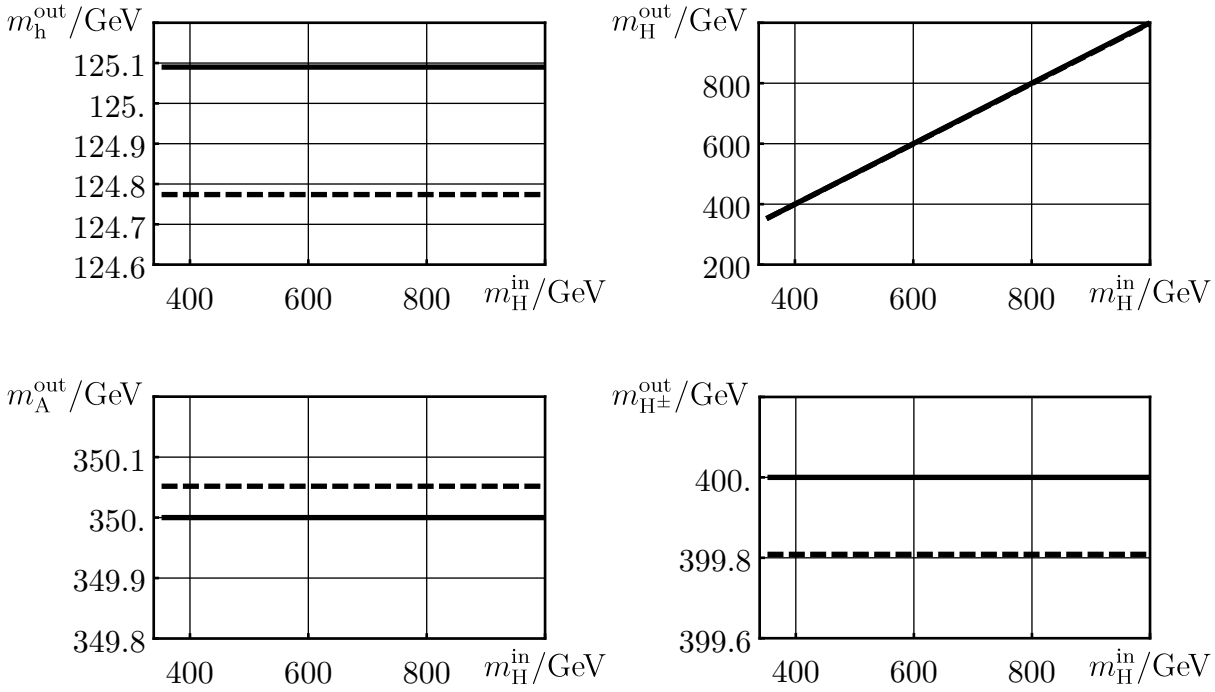

Figure 2. Tree level scan over $m_{\mathrm{H}}^{\mathrm{in}}$ with $\theta_{12} = 0$, $m_{\mathrm{h}}^{\mathrm{in}} = 125.09$ GeV, $m_{\mathrm{A}}^{\mathrm{in}} = 350$ GeV and $m_{\mathrm{H}^{\pm}}^{\mathrm{in}} = 400$ GeV. The solid line represents output from `FlexibleSUSY` and the dashed line is for `SPheno`. The outputs of masses are arranged as follows: Top left) lightest Higgs h, Top right) heavier scalar Higgs H, Bottom left) pseudoscalar Higgs A, and Bottom right) charged Higgs $H^{\pm}$.

The parameter space is widely larger as this is just a single slice at $\theta_{12} = 0$ and the interested reader can find a scan over m_{H} and θ_{12} in Appendix B, Fig. 12 to get a better view. Here we only note that the space is restricted by θ_{12} and solutions do not exist throughout the whole range. If one wants to select physical points, the same angle restricts the choices even more.

As concluding remarks on the tree level Higgs potential, we note that both packages produce consistent results with little deviations from one another and from the input values in case of `SPheno`. The differences have occurred due to differences in calculating the vacuum expectation value of the Standard Model.

3.1.2 1-Loop corrected

In this part packages at 1-loop level are compared. Flags used in this part are listed in Tables 5 and 6 and other parameters remain as at tree level. We note, that as we do not have the expressions of Z_{abcd} parameters for the 1-loop corrected case, there are no expectations of perfectly matching the input and we simply take a look at the changes with respect to the tree level. Yet, the parameters do serve as a rough guide when scanning.

Table 5. Flags in `Block FlexibleSUSY` for the loop corrected case

LesHouches	Mathematica name	Value
4	`poleMassLoopOrder`	1
5	`ewsbLoopOrder`	1

Table 6. Flag in `Block SPhenoInput` for the loop corrected case

LesHouches	Mathematica name	Value
55	`LoopMass`	1

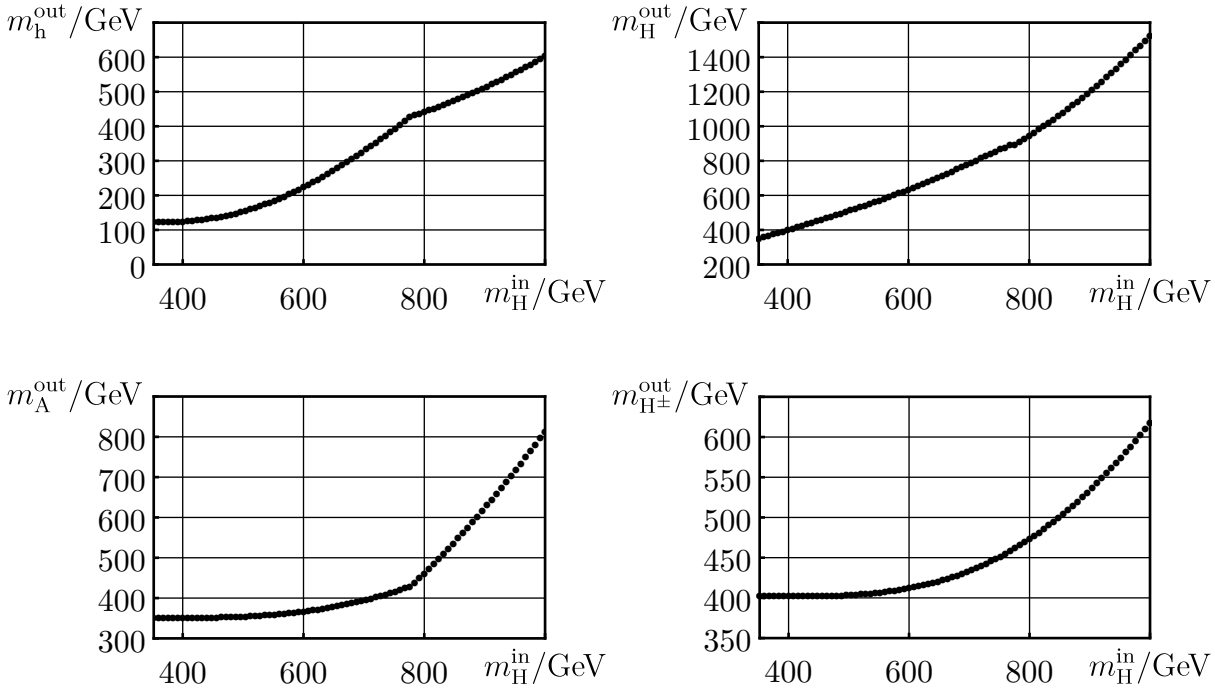

Figure 3. 1-loop level scan over $m_{\rm H}^{\rm in}$ with $\theta_{12} = 0$, $m_{\rm h}^{\rm in} = 125.09$ GeV, $m_{\rm A}^{\rm in} = 350$ GeV and $m_{\rm H^\pm}^{\rm in} = 400$ GeV. The outputs of masses are arranged as follows: Top left) lightest Higgs h, Top right) heavier scalar Higgs H, Bottom left) pseudoscalar Higgs A, and Bottom right) charged Higgs $H^\pm$. Output is from `FlexibleSUSY`

In Fig. 3 we see that the 1-loop corrected case is very different from the tree level from the previous section. Starting from the plot in the top right corner, it is clear that the input of

the mass of the heavier scalar Higgs H is no longer equal to the output mass $m_{\mathrm{H}}^{\mathrm{out}}$ through the whole range. Up to the input of 600 GeV the dependence is almost linear, but at 1000 GeV the output mass is already ≈ 400 GeV bigger than the input. Other Higgs bosons also deviate more and more as the input mass $m_{\mathrm{H}}^{\mathrm{in}}$ increases. Mass of the lightest Higgs becomes as much as 5 times the input value at the end of the range of $m_{\mathrm{H}}^{\mathrm{out}}$, mass of the pseudo scalar Higgs A is doubled by the time $m_{\mathrm{H}}^{\mathrm{out}}$ reaches 1000 GeV, while the charged Higgs additionally gains only half of the input value.

As the goal of the thesis is to compare the packages we do not dive deeply into the nature of loop corrections and instead compare how different are the outputs of packages. In Fig. 3 only the output of `FlexibleSUSY` is plotted as the scale is to big and the differences would be invisible, which is already a good sign. In order to see the differences we look at the ratios of output masses from the packages:

$$r_i = \frac{m_i^{\mathrm{FS}}}{m_i^{\mathrm{SP}}} - 1. \tag{3.1.8}$$

Here i enumerates the Higgses, m_i^{FS} is the output mass from `FlexibleSUSY`, m_i^{SP} is from `SPheno` and we subtract 1 to look just at the deviation.

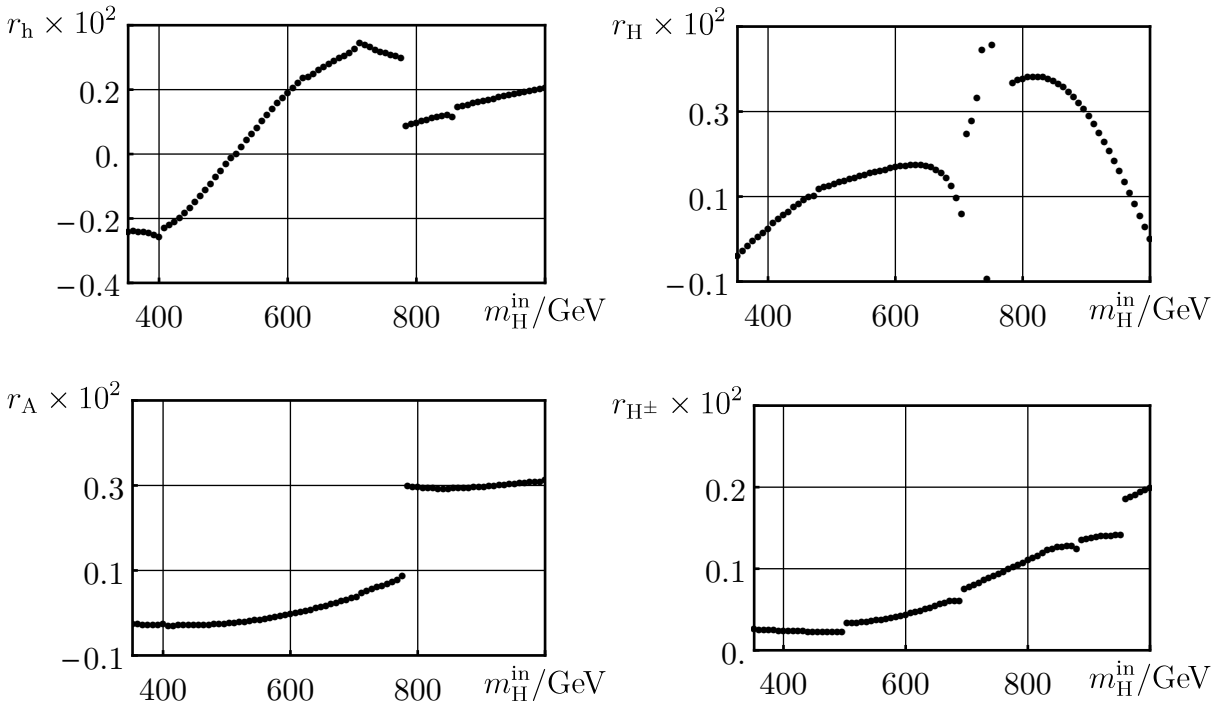

Figure 4. Higgs mass ratios r_i between `FlexibleSUSY` and `SPheno` outputs. The same scan and same layout as specified in Fig. 3.

In Fig. 4 the plots of r_i are shown. At first, we note that on vertical axes we have $r_i \times 10^2$, or percent, and in turn it means that the differences really are small — not more than a percent. However, these parts of percent can become a difference of 8 GeV between the packages for the given masses. We note, that these deviations are not caused by the vacuum expectation value in `SPheno` and plots with a different VEV can be found in Appendix B, Fig. 11. We

only state that with a different VEV for SPheno the plots change visually and SPheno outputs bigger values than FlxibleSUSY in a bigger range, but the maximum amplitude of deviation does not change. Since both packages use the same analytical 1-loop expressions from SARAH, inconsistencies could be caused by different iterative approaches. Even in FlexibleSUSY alone there are three precision regimes that use different techniques and the output masses differ. The reported deviation was around 0.3 % for a certain model at a single point and can be found in [3]. Evidently, the difference between SPheno and FlexibleSUSY is also of the same order and can be accounted to different approaches. In addition, the dependencies are fairly complicated and discontinuous as they have a lot of breaks that do not change in amount or positions when the VEV is adjusted for SPheno. These breaks could mean very slight shifts of some bending points between packages, as the one near 800 GeV mark in Fig. 3 in plots of $m_{\mathrm{h}}^{\mathrm{out}}$ and $m_{\mathrm{H}}^{\mathrm{out}}$.

Even though we are unable to adequately compare input and output at 1-loop level, we are still able to see that the output of FlexibleSUSY and SPheno differs by up to 0.5%.

3.2 Neutrino sector

As mentioned above, SPheno breaks down with complex Yukawa couplings and it is impossible to compare FlexibleSUSY and SPheno in the neutrino sector. However, we can see how the output of FlexibleSUSY compares to neutrino data, namely the expected neutrino masses and the PMNS matrix. While masses of neutrinos are briefly inspected at tree level and in full with 1-loop corrections, we take a look at the PMNS matrix only at 1-loop level. The flags for tree level and 1-loop corrected cases are the same as in the Higgs sector.

3.2.1 Neutrino mass outputs

For the tree level we only want to check one feature of the model and whether FlexibleSUSY is able to reproduce it. As mentioned in Sections 1.4.3 and 1.4.4, at tree level there are two massless neutrinos and we try to see if this feature is existent.

In Fig. 5 the two lower plots nicely show the heavy state with the mass $m_4 \sim M_{\mathrm{R}}$ as well as the massive state m_3 already at $\sim 10^{-11}$ GeV and near the expected value from Eq. (1.4.59). Two upper plots show very small and random numbers at $\sim 10^{-20}$ GeV, which mean nothing more but a numerical zero. In other words, the tree level property of the Grimus-Neufeld model is reproduced by FlexibleSUSY. We only note here that for this check we did a scan over the Higgs sector, used the 1-loop corrected relations in the neutrino sector, and did not have the intention to hit any physical points. Input parameters used at tree level are specified in the caption of Fig. 5.

With one loop corrections included we want to reproduce more properties than just the amount of massless neutrinos. To be able to probe the neutrino sector at 1-loop level, unlike at tree level, we first need to select a working point for the Higgs potential. As seen in the previous section, the parameters of the Higgs potential give out masses that are off by a huge margin from the input values when loop corrections are included. To achieve consistency between values

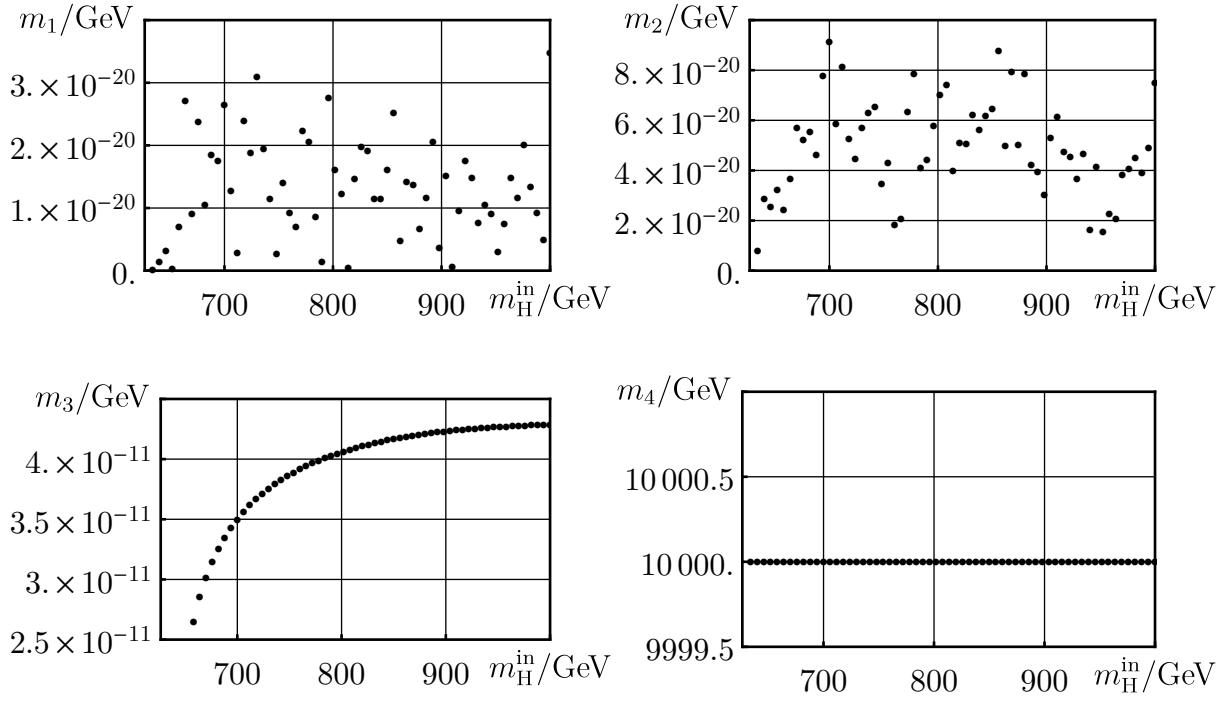

Figure 5. Masses of neutrinos at tree level, while scanning over the mass of H boson. The parameter point is as follows: $m_{\rm h}^{\rm in} = 125.09$ GeV, $m_{\rm A}^{\rm in} = 350$ GeV, $m_{\rm H^\pm}^{\rm in} = 450$ GeV, $\theta_{12}^{\rm in} = \frac{\pi}{2}$, $M_{\rm R} = 10^4$, $\lambda_{\rm D} = 0.9$, $\phi = \frac{\pi}{2}$.

used internally in `FlexibleSUSY` and the values we use in calculations of the neutrino sector parameters, we first scan over the Higgs potential and select points where the lightest Higgs has the mass of 125 GeV within 3 GeV. In addition, we have

$$\begin{aligned} m_{\rm H^\pm} &> 400 \text{ GeV}, \\ m_{\rm H^\pm} - m_{\rm A} &> 8 \text{ GeV and} \\ m_{\rm H} - m_{\rm A} &> 8 \text{ GeV} \end{aligned} \tag{3.2.1}$$

to be consistent with [34]. At selected points we take Z_{abcd} parameters and the output masses of Higgses. When scanning over the neutrino sector, the potential parameters go directly into the potential without any recalculation and the output masses are used in calculations of the neutrino sector parameters. This way we are able to be consistent at 1-loop level between what we put in and what the software uses internally.

However, there is one parameter, θ_{12}, that needs a little extra work. Additional effort is needed, because θ_{12} is not part of the usual `FlexibleSUSY` output parameters and needs to be calculated from the Higgs mixing matrix. This matrix, $U_{\rm ZH}$, was only briefly mentioned in the coursework when defining the `MatterSector` in `SARAH`. $U_{\rm ZH}$ is a 4×4 matrix that mixes the scalar and pseudoscalar parts of Higgs doublets into physical Higgses. In addition to h, A and H, the Higgs multiplet also contains the Goldstone boson that is absorbed into the Z boson. Because we have chosen to deal with the real case, where the scalar and pseudo scalar parts do

not mix, the matrix U_{ZH} has a calculations-friendly form:

$$U_{\mathrm{ZH}} = \begin{pmatrix} 0 & 0 & \cos\theta_{34} & \sin\theta_{34} \\ \cos\theta_{12} & \sin\theta_{12} & 0 & 0 \\ -\sin\theta_{12} & \cos\theta_{12} & 0 & 0 \\ 0 & 0 & -\sin\theta_{34} & \cos\theta_{34} \end{pmatrix} \tag{3.2.2}$$

Here θ_{34} is the angle that mixes pseudo scalar parts. From the matrix it is easily seen that we only need to take $\arcsin(U_{ZH})_{22}$ to get the angle θ_{12}. For the neutrino sector we have selected to analyze two points with noticeably different masses of the heavier scalar H boson. The points are specified in Tables 7 and 8. Masses are given in GeV, θ_{12} in radians, M_{222} in GeV^2 and the quartic couplings are dimensionless.

Table 7. Higgs potential parameters of working points p_1 and p_2

Point	Z_{1111}	Z_{2222}	Z_{2211}	Z_{2112}	Z_{2121}	Z_{1112}	Z_{2212}	M_{222}
p_1	0.193934	0.27	1	-0.748326	-0.244401	0.540498	0	129 688
p_2	3.43181	0.27	1	-0.927979	-0.154575	3.69926	0	129 688

Table 8. Physical parameters of working points p_1 and p_2 used during the pre-calculation phase for the neutrino sector

Point	m_{h}	m_{A}	m_{H}	$m_{\mathrm{H}^\pm}$	θ_{12}
p_1	125.72	365.072	391.43	402.421	0.295065
p_2	126.568	390.574	1033.99	417.703	1.14823

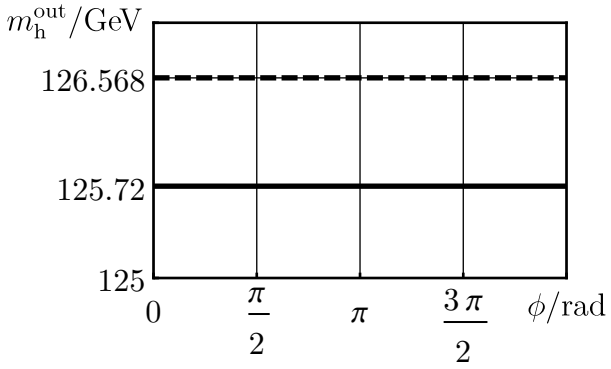

Figure 6. Output masses of h bosons when scanning over the phase ϕ of the d' parameter. The solid line represents p_1 and the dashed line represents p_2 parameter points of the Higgs potential. $M_{\mathrm{R}} = 10^4$ GeV and $\lambda_D = 1.3$

To justify our approach for having consistent calculations we check whether the mass of the lightest Higgs stays the same throughout the range of scanning, the output can be seen in Fig. 6. Ticks on the vertical axis denote the numerical input values, to better see if the output matches.

Obviously, the output perfectly matches our input for both points and because of that we also get the same mixing angle θ_{12}. In other words, our procedure worked out.

Just like at tree level, we check the number of massless neutrinos in Fig. 7, where we scan over the phase ϕ, set $M_{\rm R} = 10^4$ GeV and $\lambda_D = 1.3$. It is easily seen that we get one massless state (top left plot), two light neutrinos and one heavy neutrino as predicted at both working points p_1 and p_2. We note that the masses of light neutrinos noticeably differ at different Higgs sector parameter points. However, none of the points become small enough as they are still missing a desired factor of 10^{-1}.

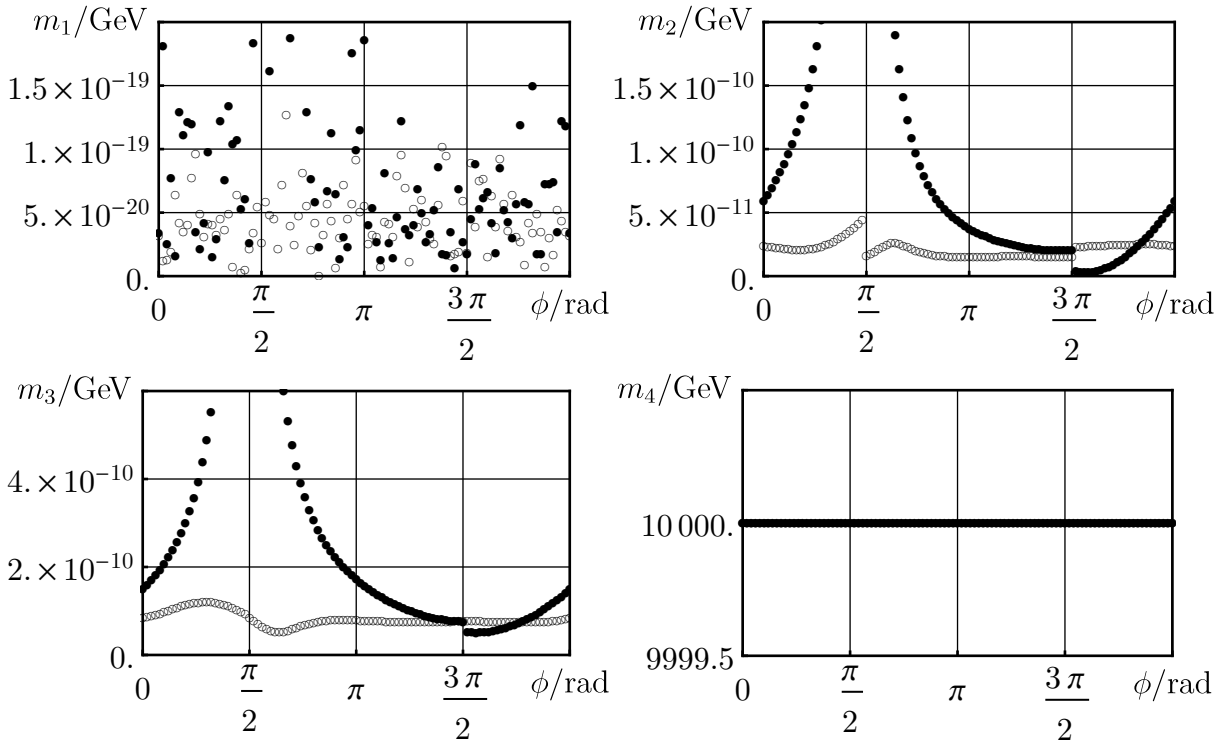

Figure 7. Output masses of neutrinos when scanning over the phase ϕ of the d' parameter. Filled circles represent the point p_1 and empty circles represent the point p_2 of Higgs parameters. $M_{\rm R} = 10^4$ GeV and $\lambda_{\rm D} = 1.3$

We try to find more suitable parameter points by selecting a few different values of the seesaw scale, $M_{\rm R}$, and seeing what changes. In Fig. 8 we look at the output masses of the two light neutrinos m_2 and m_3. In the two upper plots, that are produced at the parameter point p_1, the masses of neutrinos do not get down to the desired values. For m_2 the mass does not reach the 10^{-12} GeV mark and m_3 does not fall below 10^{-11} GeV. However, the situation is quite different at the point p_2. The output mass m_3 does fall below 10^{-11} GeV while m_2 gets closer to, but does not cross, the wanted threshold. When comparing the two points: p_1 and p_2, it is seen that qualitatively the mass outputs look different, in addition, the parameter space becomes restricted at the point p_2 for $M_{\rm R} = 10^5$ GeV and $M_{\rm R} = 10^6$ GeV. The breaks in these plots are most probably brought in by $|d'|$, when solving the 4th order polynomial and filtering the unwanted or alternative solutions as there can be 4 of them. It could be that at $\frac{\pi}{2}$ and $\frac{3\pi}{2}$ there is a switch to another branch of solutions and that causes the breaks, however, mass functions

remain 2π-symmetric.

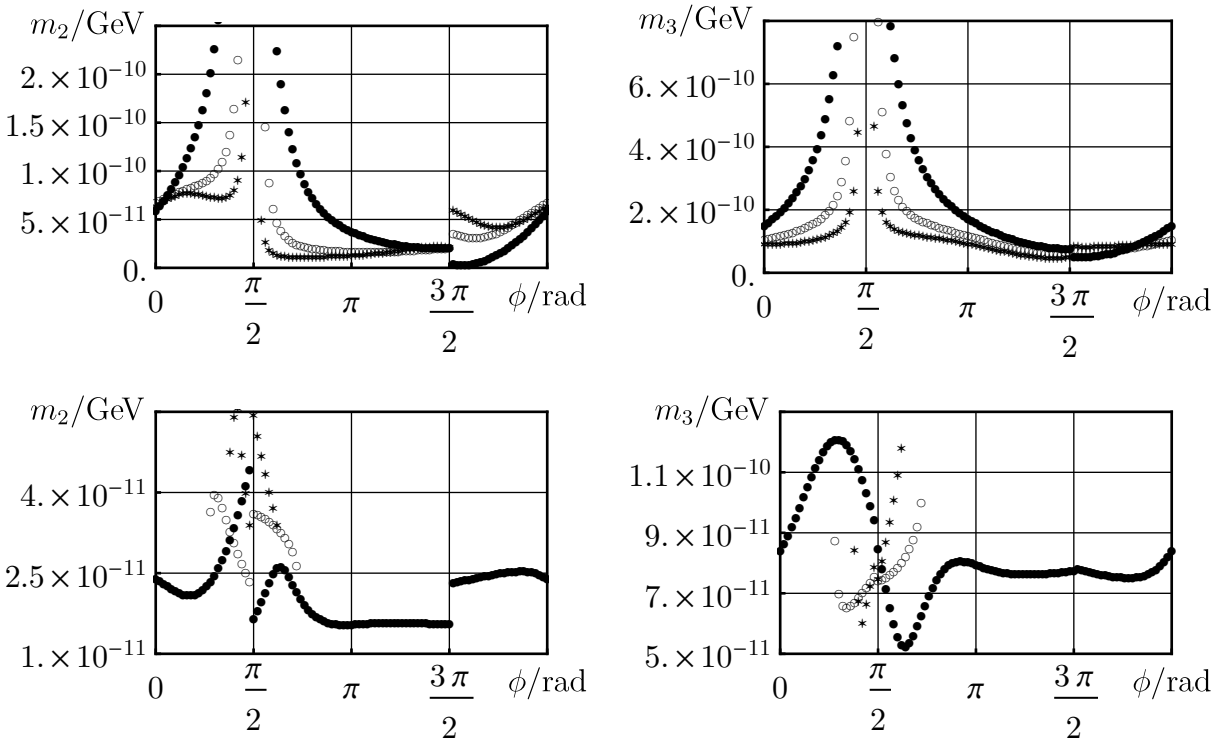

Figure 8. Output masses of neutrinos when scanning over the phase ϕ of the d' parameter. For filled circles $M_{\rm R} = 10^4$ GeV, for empty circles $M_{\rm R} = 10^5$ GeV and stars represent $M_{\rm R} = 10^6$ GeV. In all cases $\lambda_{\rm D} = 1.3$. Two upper plots are for the parameter point p_1 and the two lower plots are for the parameter point p_2

We also try lower values of $M_{\rm R}$ and start looking from 200 GeV to 10^3 GeV with the step of 100 GeV. For the parameter point p_1 `FlexibleSUSY` gives output at the lowest of $M_{\rm R} = 900$ GeV, while at p_2 the lowest value is $M_{\rm R} = 200$ GeV. However, the next smallest $M_{\rm R}$ value to produce output at p_2 is $M_{\rm R} = 10^4$ GeV. In addition to the strangely separated lowest value, the outputs of neutrino masses are $2-3$ orders of magnitude lower than at p_1 and the parameter space is restricted to $\pi < \phi < 2\pi$. All of this can be seen in Fig. 9.

Evidently, this proves that `FlexibleSUSY` is able to calculate neutrino masses at the required order of $10^{-11} - 10^{-12}$ GeV even with double precision. Also, theoretical properties of neutrino masses were reproduced: two massless states at tree level, only one massless state with 1-loop corrections and one heavy state with $m_4 \approx M_{\rm R}$ in both cases. However, we were not able to pin down parameter points where both of the neutrino masses are as expected, but that is a matter of complexity of the parameter space and made assumptions.

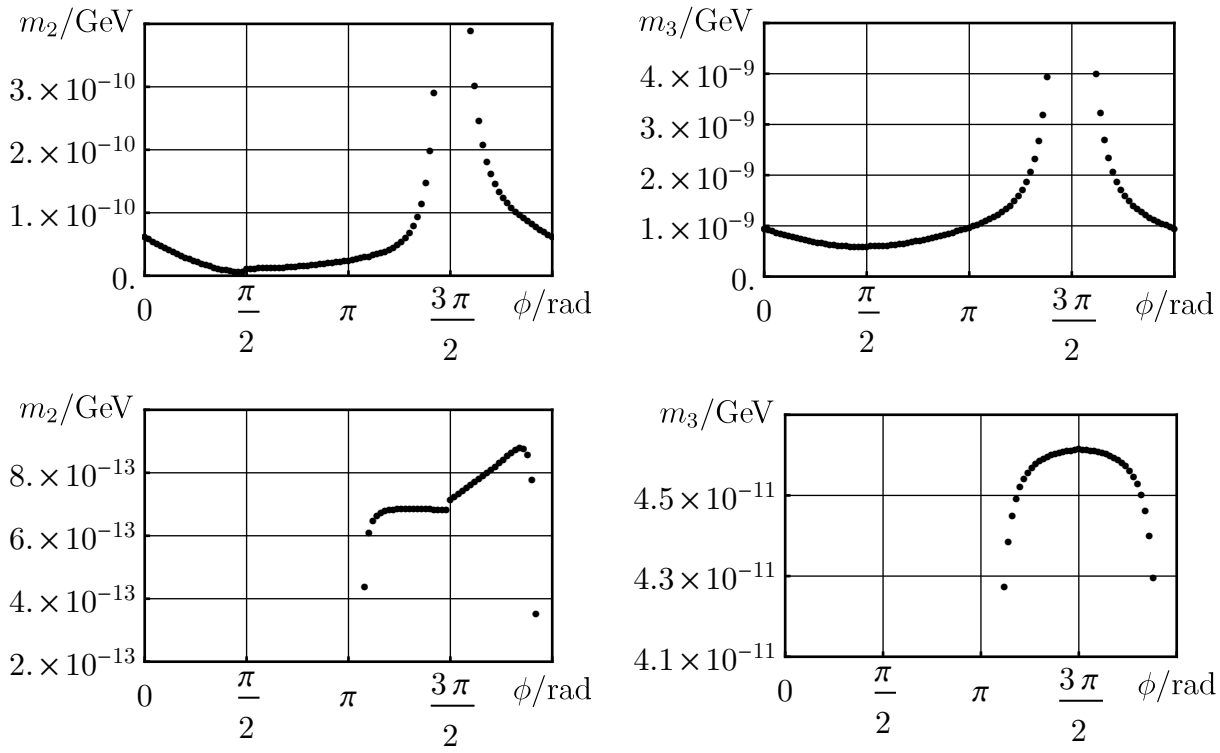

Figure 9. Mass outputs of light neutrino states m_2 and m_3 when scanning over the phase ϕ with $\lambda_D = 1.3$. Two upper plots are for the parameter point p_1 and have $M_{\rm R} = 900$ GeV, the lower plots are for p_2 and have $M_{\rm R} = 200$ GeV.

3.2.2 Comparison of PMNS matrices

Before concluding the thesis we do a brief comparison of the measured PMNS matrix and the one we get as output from `FlexibleSUSY`.

For the comparison we take the lowest point from the bottom right plot in Fig. 7 with $M_{\rm R} = 10^4$ GeV. At that point the mass m_4 of the heavier light neutrino is equal to 5.255×10^{-11} GeV, which is close to the desired value of 5.124×10^{-11} GeV, while $m_3 = 2.628 \times 10^{-11}$ GeV and is a bit off from the expected value of 8.695×10^{-12} GeV. Nonetheless, it makes sense to select this point for the comparison, as the masses are quite close to the expected values, which are based on the measured mass differences squared and the assumption of a massless neutrino.

For the measured PMNS matrix we choose the parametrization from [23]:

$$\begin{aligned} \theta_{12} &= 34.5 \ \text{deg}, \\ \theta_{13} &= 8.44 \ \text{deg}, \\ \theta_{23} &= 41 \ \text{deg}, \\ \delta &= 0 \ \text{deg}\,. \end{aligned} \tag{3.2.3}$$

Here θ_{ij} are parameters of the PMNS matrix and should not be confused with the Higgs sector parameters, δ is the phase and, as mentioned previously, it is set to 0 due to big uncertainties. With this parametrization the resulting PMNS matrix is real, but the matrix that we get from `FlexibleSUSY` is complex, therefore we will compare absolute values of matrix elements.

Before writing down the measured matrix we note a few things about the matrix from `FlexibleSUSY`. First of all, the matrix that we get at the specified point is:

$$\begin{pmatrix} 0.806 - \mathrm{i}0.123 & -0.501 + \mathrm{i}0.077 & 0.277 - \mathrm{i}0.042 & (-5.31 + \mathrm{i}9.52) \times 10^{-14} \\ 0.084 + \mathrm{i}0.425 & -0.421 + \mathrm{i}0.473 & -0.516 - \mathrm{i}0.381 & (-3.18 - \mathrm{i}0.78) \times 10^{-8} \\ 0.316 - \mathrm{i}0.219 & 0.172 - \mathrm{i}0.559 & -0.608 - \mathrm{i}0.375 & (0.07 - \mathrm{i}8.86) \times 10^{-8} \\ (1.90 + \mathrm{i}1.37) \times 10^{-8} & (5.94 - \mathrm{i}0.34) \times 10^{-8} & (5.22 - \mathrm{i}4.60) \times 10^{-8} & -1 + \mathrm{i}10^{-17} \end{pmatrix} \tag{3.2.4}$$

Here we see that by neglecting small numbers the matrix easily reduces to the block diagonal form mentioned in Sec. 1.4.3, Eq.(1.4.42). Though, the matrix did pick up a minus sign in the bottom right corner element, which is a matter of definitions and can be ignored. For the comparison to the measured PMNS matrix we use the reduced 3×3 block of this matrix and take absolute values of matrix elements:

$$V_{\mathtt{FS}}^{\mathrm{PMNS}} = \begin{pmatrix} 0.815 & 0.507 & 0.280 \\ 0.433 & 0.633 & 0.642 \\ 0.384 & 0.585 & 0.714 \end{pmatrix}. \tag{3.2.5}$$

We now also write down the measured PMNS matrix and remind that the absolute values of elements are shown:

$$V_{\mathrm{meas.}}^{\mathrm{PMNS}} = \begin{pmatrix} 0.815 & 0.560 & 0.147 \\ 0.507 & 0.567 & 0.649 \\ 0.280 & 0.603 & 0.747 \end{pmatrix}. \tag{3.2.6}$$

Evidently, the matching is quite good, as the elements of matrices $V_{\mathtt{FS}}^{\mathrm{PMNS}}$ and $V_{\mathrm{meas.}}^{\mathrm{PMNS}}$ do not differ by more than 0.133, while, for example, the element $\left(V_{\mathrm{meas.}}^{\mathrm{PMNS}}\right)_{11}$ matches exactly at shown accuracy. On the other hand, we do not expect to have a perfect match as there are assumptions in the model, uncertainties in the measured mass square differences and the measured PMNS matrix, which are not negligible. In addition, if we wanted to improve the agreement of measurements and calculations, we would also have to include the phase δ, which is poorly measured at the moment and was ignored. In other words, this level of matching is enough to show that `FlexibleSUSY` is sufficient and gives consistent output.

Conclusions

To conclude, during the thesis we have achieved quite a few results:

1. We dealt with all of the practical problems with software packages to fully implement the Grimus-Neufeld model and that included:
   - refining the `SARAH` model file for the Grimus-Neufeld model,
   - overcoming bugs and finishing the model implementation in `FlexibleSUSY`,
   - figuring out problems behind quadruple precision and masses of neutrinos in `SPheno`,
   - writing a `Mathematica` package, `SSS`, for doing parameter scans with `SPheno` as the original package was not sufficient for our needs, when calculating theoretical parameters from physical input,
   - figuring out correct flags for doing parameter scans in both packages.
2. In the Higgs sector and at tree level we were able to get back masses of Higgses that we put in from the output and to show that quantitatively `FlexibleSUSY` and `SPheno` behave exactly the same, whereas numerically the difference lies in `SPheno` internally using a slightly different numerical value of the vacuum expectation value, and therefore, showing a deviation from physical input and output of `FlexibleSUSY`.
3. At 1-loop level in the Higgs sector we have found that the deviation in our performed scan was at most 0.5% between packages independently of the vacuum expectation value used internally in `SPheno` and the deviation was amounted to different iterative approaches, as both spectrum generators use analytical expressions for 1-loop corrections from `SARAH`.
4. In the neutrino sector, when using a parametrization that results in complex Yukawa couplings, it is only possible to compare `FlexibleSUSY` to theoretical and experimental expectations, as `SPheno` uses other methods of matrix diagonalization to find mass eigenvalues and is numerically unable to deal with the neutrino sector.
5. At tree level and with 1-loop corrections included in the neutrino sector `FlexibleSUSY` is able to reproduce the correct amount of massless neutrino states in the Grimus-Neufeld model: 2 at tree level and 1 at 1-loop level.
6. `FlexibleSUSY` is able to calculate masses down to the order of 10^{-13} GeV, which is enough for neutrinos in the Grimus-Neufeld model.
7. The measured PMNS matrix and the PMNS matrix from `FlexibleSUSY` output matches to a satisfactory level, when the uncertainties of neutrino data and assumptions of the Grimus-Neufeld model are considered.

References

[1] W. Grimus and H. Neufeld. “Radiative neutrino masses in an SU(2) $\times$ U(1) model”. In: *Nuclear Physics B* 325.1 (1989), pp. 18 –32. ISSN: 0550-3213. DOI: https://doi.org/10.1016/0550-3213(89)90370-2.

[2] S. Draukšas. *Automatizing the Grimus-Neufeld model*. Course work of the Physics bachelor study program. Supervisor doc. dr. Thomas Gajdosik. Vilnius: Physics faculty of Vilnius university, 2018, 39 pages.

[3] P. Athron et al. “FlexibleSUSY—A spectrum generator generator for supersymmetric models”. In: *Comput. Phys. Commun.* 190 (2015), pp. 139–172. DOI: 10.1016/j.cpc.2014.12.020. arXiv: 1406.2319 [hep-ph].

[4] P. Athron et al. “FlexibleSUSY 2.0: Extensions to investigate the phenomenology of SUSY and non-SUSY models”. In: (2017). arXiv: 1710.03760 [hep-ph].

[5] B. C. Allanach. “SOFTSUSY: a program for calculating supersymmetric spectra”. In: *Comput. Phys. Commun.* 143 (2002), pp. 305–331. DOI: 10.1016/S0010-4655(01)00460-X. arXiv: hep-ph/0104145 [hep-ph].

[6] B. C. Allanach et al. “Next-to-Minimal SOFTSUSY”. In: *Comput. Phys. Commun.* 185 (2014), pp. 2322–2339. DOI: 10.1016/j.cpc.2014.04.015. arXiv: 1311.7659 [hep-ph].

[7] W. Porod. “SPheno, a program for calculating supersymmetric spectra, SUSY particle decays and SUSY particle production at e^+e^- colliders”. In: *Comput. Phys. Commun.* 153 (June 2003), pp. 275–315. DOI: 10.1016/S0010-4655(03)00222-4. eprint: hep-ph/0301101.

[8] W. Porod and F. Staub. “SPheno 3.1: Extensions including flavour, CP-phases and models beyond the MSSM”. In: *Comput. Phys. Commun.* 183 (2012), pp. 2458–2469. DOI: 10.1016/j.cpc.2012.05.021. arXiv: 1104.1573 [hep-ph].

[9] M. B. Robinson. *Symmetry and the Standard Model. Mathematics and Particle Physics*. 1. Springer-Verlga New York, 2011, pp. XIX, 327. DOI: 10.1007/978-1-4419-8267-4.

[10] M. B. Robinson, T. Ali, and G. B. Cleaver. “A Simple Introduction to Particle Physics Part II”. In: *ArXiv e-prints* (Aug. 2009). arXiv: 0908.1395 [hep-th].

[11] J. Goldstone. “Field theories with "superconductor" solutions”. In: *Nuovo Cimento* 19.CERN-TH-118 (1960), pp. 154–164. URL: http://cds.cern.ch/record/343400.

[12] S. Scherer and M. R. Schindler. *A Primer for Chiral Perturbation Theory*. 1. Springer-Verlga Berlin Heidelberg, 2012, pp. IX, 338. DOI: 10.1007/978-3-642-19254-8.

[13] S. Weinberg. “Physical Processes in a Convergent Theory of the Weak and Electromagnetic Interactions”. In: *Physical Review Letters* 27 (Dec. 1971), pp. 1688–1691. DOI: 10.1103/PhysRevLett.27.1688.

[14] S. Weinberg. “General Theory of Broken Local Symmetries”. In: *Physical Review D* 7 (Feb. 1973), pp. 1068–1082. DOI: 10.1103/PhysRevD.7.1068.

[15] Mark Srednicki. *Quantum Field Theory*. Cambridge: Cambridge Univ. Press, 2007. URL: https://cds.cern.ch/record/1019751.

[16] P. Langacker. *The standard model and beyond*. Series in High Energy Physics, Cosmology and Gravitation. Boca Raton, FL: Taylor and Francis, 2010. URL: https://cds.cern.ch/record/1226768.

[17] C. Patrignani et al. “Review of Particle Physics”. In: *Chin. Phys.* C40.10 (2016), p. 100001. DOI: 10.1088/1674-1137/40/10/100001.

[18] H. E. Haber and D. O’Neil. “Basis-independent methods for the two-Higgs-doublet model. III. The CP-conserving limit, custodial symmetry, and the oblique parameters S, T, U”. In: *Physical Review D* 83.5, 055017 (Mar. 2011), p. 055017. DOI: 10.1103/PhysRevD.83.055017. arXiv: 1011.6188 [hep-ph].

[19] P. B. Pal. “Dirac, Majorana, and Weyl fermions”. In: *American Journal of Physics* 79 (May 2011), pp. 485–498. DOI: 10.1119/1.3549729. arXiv: 1006.1718 [hep-ph].

[20] Z. Maki, M. Nakagawa, and S. Sakata. “Remarks on the Unified Model of Elementary Particles”. In: *Progress of Theoretical Physics* 28 (Nov. 1962), pp. 870–880. DOI: 10.1143/PTP.28.870.

[21] B. Pontecorvo. “Inverse beta processes and nonconservation of lepton charge”. In: *Sov. Phys. JETP* 7 (1958). [Zh. Eksp. Teor. Fiz.34,247(1957)], pp. 172–173.

[22] *Private communication with the supervisor doc. dr. T. Gajdosik.*

[23] P. F. de Salas et al. “Status of neutrino oscillations 2018: first hint for normal mass ordering and improved CP sensitivity”. In: (2017). arXiv: 1708.01186 [hep-ph].

[24] F. Staub. “From Superpotential to Model Files for FeynArts and CalcHep/CompHep”. In: *Comput. Phys. Commun.* 181 (2010), pp. 1077–1086. DOI: 10.1016/j.cpc.2010.01.011. arXiv: 0909.2863 [hep-ph].

[25] F. Staub. “Automatic Calculation of supersymmetric Renormalization Group Equations and Self Energies”. In: *Comput. Phys. Commun.* 182 (2011), pp. 808–833. DOI: 10.1016/j.cpc.2010.11.030. arXiv: 1002.0840 [hep-ph].

[26] F. Staub. “SARAH 3.2: Dirac Gauginos, UFO output, and more”. In: *Comput. Phys. Commun.* 184 (2013), pp. 1792–1809. DOI: 10.1016/j.cpc.2013.02.019. arXiv: 1207.0906 [hep-ph].

[27] F. Staub. “SARAH 4 : A tool for (not only SUSY) model builders”. In: *Comput. Phys. Commun.* 185 (2014), pp. 1773–1790. DOI: 10.1016/j.cpc.2014.02.018. arXiv: 1309.7223 [hep-ph].

[28] Peter Z. Skands et al. “SUSY Les Houches accord: Interfacing SUSY spectrum calculators, decay packages, and event generators”. In: *JHEP* 07 (2004), p. 036. DOI: 10.1088/1126-6708/2004/07/036. arXiv: hep-ph/0311123 [hep-ph].

[29] SARAH Forum. http://sarah.hepforge.org/forum.html.

[30] *Private communication with dr. A. Voigt and dr. P. Athron.*

[31] *Private communication with dr. F. Staub.*

[32] Alexander M. Chebotarev and Alexander E. Teretenkov. “Singular value decomposition for the Takagi factorization of symmetric matrices”. In: *Applied Mathematics and Computation* 234 (2014), pp. 380 –384. ISSN: 0096-3003. DOI: https://doi.org/10.1016/j.amc.2014.01.170. URL: http://www.sciencedirect.com/science/article/pii/S0096300314002239.

[33] F. Staub et al. “A tool box for implementing supersymmetric models”. In: *Comput. Phys. Commun.* 183 (Oct. 2012), pp. 2165–2206. DOI: 10.1016/j.cpc.2012.04.013. arXiv: 1109.5147 [hep-ph].

[34] A. Belyaev et al. “Anatomy of the Inert Two Higgs Doublet Model in the light of the LHC and non-LHC Dark Matter Searches”. In: *Physical Review* D97.3 (2018), p. 035011. DOI: 10.1103/PhysRevD.97.035011. arXiv: 1612.00511 [hep-ph].

[35] T. Gajdosik, A. Juodagalvis, and D. Jurčiukonis. “The loop improved Yukawa couplings of the Grimus-Neufeld model”. In: Conference:LNFK42. 2017.

[36] T. Plehn and M. Rauch. “Quartic Higgs coupling at hadron colliders”. In: *"Physical Review"* D72.5, 053008 (Sept. 2005), p. 053008. DOI: 10.1103/PhysRevD.72.053008. eprint: hep-ph/0507321.

[37] F. Staub and W. Porod. “Improved predictions for intermediate and heavy supersymmetry in the MSSM and beyond”. In: *European Physical Journal C* 77, 338 (May 2017), p. 338. DOI: 10.1140/epjc/s10052-017-4893-7. arXiv: 1703.03267 [hep-ph].

Santrauka

SPheno ir FlexibleSUSY palyginimas Grimus-Neufeld modelyje

Simonas Draukšas

Šiame darbe palyginami du programiniai paketai — spektrų generatoriai: FlexibleSUSY ir SPheno, į juos suvedant Grimus-Neufeld modelį ir palyginant teorinius modelio bruožus, eksperimentinius duomenis bei programinių paketų išvestį.

Teorinėje dalyje pateikta bendra ir reikalinga dalelių fizikos teorija, aprašytos pagrindinės Grimus-Neufeld modelio dalys, jų veikimo principas, modelyje esantys teoriniai bei atitinkami fizikiniai parametrai, taip pat trumpai pristatomi naudoti programiniai paketai ir jų paskirtis.

Antrojoje dalyje aprašoma po kursinio darbo likusi modelio suvedimo į spektrų generatorius proceso dalis. Išsprendžiamos problemos kilusios FlexibleSUSY dėl kompleksinių parametrų aprašymo, potencialo minimumo sprendinių bei dėl klaidų pačiame programiniame pakete, pateikiamas parametrų skenavimo procesas. Taip pat nurodyti pakeitimai, kuriuos reikia atlikti SPheno modelio faile, norint skaičiuoti neutrinų mases. Tačiau net ir atlikus pakeitimus dėl SPheno naudojamų metodų iškyla skaitmeninių problemų ir neutrinų masių neįmanoma apskaičiuoti Grimus-Neufeld modelyje, kai naudojami kompleksiniai parametrai. Kadangi standartinio SSP paketo, skirto parametrų skenavimui su SPheno, nepakanka reikalingiems fizikinių parametrų perskaičiavimams į teorinius, buvo parašytas specialus paketas SSS, kurio trumpas aprašymas taip pat pateikiamas šioje dalyje.

Trečiojoje dalyje atliekamas programinių paketų palyginimas, kuris suskirstytas į dvi pagrindines dalis: Higgs'o ir neutrinų sektorius. Higgs'o sektoriuje nagrinėjamas tik Higgs'o potencialas prilyginus Yukawos sąveikas su neutrinais nuliui. Iš pradžių palyginimas daromas medžio lygmenyje (angl. *tree level*), kuriame tikriname teorinių Higgs'o potencialo formulių atitikimą su paketų išvestimi, o taip pat ir paketų tarpusavio išvestį. Gautas atitikimas tarp fizikinių parametrų įvesties ir FlexibleSUSY išvesties, o SPheno išvestis šiek tiek skyrėsi dėl skirtingos skaitmeninės vakuumo reikšmės (angl. *vacuum expectation value*) paketo viduje. Įskaičius vienos kilpos pataisas (angl. *1-loop correction*) Higgs'o sektoriuje programų išvestis buvo palyginta tarpusavyje naudojant apibrėžtą santykį r_i ir gautas skirtumas tarp programų neviršijo 0.5%.

Neutrinų sektoriuje, medžio lygmenyje įsitikinta, jog FlexibleSUSY atkartoja teisingą masyvių ir bemasių neutrinų skaičių. Tolimesni patikrinimai atlikti ties vienos kilpos lygmeniu, kadangi turimi neutrinų sektoriaus parametrai aprašyti būtent ties šiuo lygmeniu. Darbe parodyta, jog įskaičius vienos kilpos pataisas FlexibleSUSY atkartoja teisingą masyvių ir bemasių neutrinų skaičių, be skaitmeninių sunkumų gali gauti mases net iki 10^{-13} GeV. Taip pat parodyta, jog pasirinktame parametrų taške iš FlexibleSUSY gaunama neutrinų maišymosi matrica, kuri yra pakankamai panaši į išmatuotą PMNS matricą.

Appendices

A Constant flags in FlexibleSUSY and SPheno

Flags used in all scans with FLexibleSUSY in Block FlexibleSUSY:

Table 9. Flags in Block FlexibleSUSY

LesHouches	Mathematica name	Value
0	precisionGoal	10^{-4}
1	maxIterations	0
2	solver	0
3	calculateStandardModelMasses	1
6	betaFunctionLoopOrder	0
7	thresholdCorrectionsLoopOrder	0
$8-11$	higgs2loopCorrection<...>	0
12	forceOutput	0
13	topPoleQCDCorrections	2
14	betaZeroThreshold	10^{-11}
16	forcePositiveMasses	1
17	poleMassScale	0
$18-22$	eft<...>	Not applicable
23	calculateBSMMasses	1
$25-29$	higgs3loopCorrection<...>	0
30	higgs4loopCorrectionAtAsAsAs	0

Flags used in all scans with SPheno in Block SPhenoInput:

Table 10. Flags in Block SPhenoInput

LesHouches	Mathematica name	Value	LesHouches	Mathematica name	Value
1	Errorlvl	0	50	PositivMass	1
2	-	0	51	CKMbasis	0
7	TLHiggsCorr	1	52	TachyonicState	0
9	Gaugeless	1	57	LowEnergyConstr	0
10	SafeMode	0	61	RunningParam	0
19	ThreshLoop	0	62	RGESMRunningObs	0
34	MassPrec	10^{-4}	63	RGERunningObs	0
35	MaxIterNum	40	65	TadSolut	1
36	IterDiscardNum	5	66	TwoScaleMatch	1
37	YukawaScheme	4	67	effHiggsMass	1
38	RGELoop	0	520	EffHiggsCoup	1

SPheno also has a few specific settings in the Block MODSEL:

Table 11. Flags in Block MODSEL, in SPheno

LesHouches	Mathematica name	Value
1	LowIn	0
2	BoundaryCond	1
5	CP	2
6	-	1
12	ScaleQ	126

The implementation of parameter output scale differs a bit between packages, but the parameter output scale is set to 126 GeV in both packages. Second flag in Table 10 is not appointed a flag name and is responsible for using conventions where the parameter output scale is 1000 GeV, this is turned off by setting the flag to 0. Output scale of masses is equal to masses at poles.

For both packages we have matched their Block SMINPUTS with the values listed in [17] and they are specified in Table 12. GF is the reduced Fermi's constant, alphaSMZ is the strong force coupling constant, MZ is the pole mass of the Z boson, mbmb is the runnning mass of the bottom quark, Mt and Mtau are the pole masses of the top quark and tau lepton respectively. Masses are written in GeV, Fermi's constant has units of GeV^{-2} and strong force coupling is dimensionless. As these flags were not assigned a name in Mathematica for SPheno, the table corresponds to names used in FlexibleSUSY. In addition, FlexibleSUSY requires a lot more inputs in the Block SMINPUTS, but these are left at default values as there is no way to compare with SPheno. Though, we do set the masses of neutrinos to the ones we expect to get in FlexibleSUSY.

Table 12. Flags in Block SMINPUTS

LesHouches	Mathematica name (FS)	Value
2	GF	1.1663787×10^{-5}
3	alphaSMZ	0.1182
4	MZ	91.1876
5	mbmb	4.18
6	Mt	173.1
7	Mtau	1.77686

B Additional parameter scans

In Sec. 3.1.1, Fig. 2 we show that the difference between the physical input and output of `SPheno` is up to 0.3 GeV, while the output from `FlexibleSUSY` perfectly matches the physical input, when the numerical value of the vacuum expectation value is 246.22 GeV for both packages. In the figure below we show that, by adjusting the VEV used in `SPheno` to 245.6 GeV, we are able to reduce the difference between packages and, in turn, between output and physical input. Further settings are specified in the package.

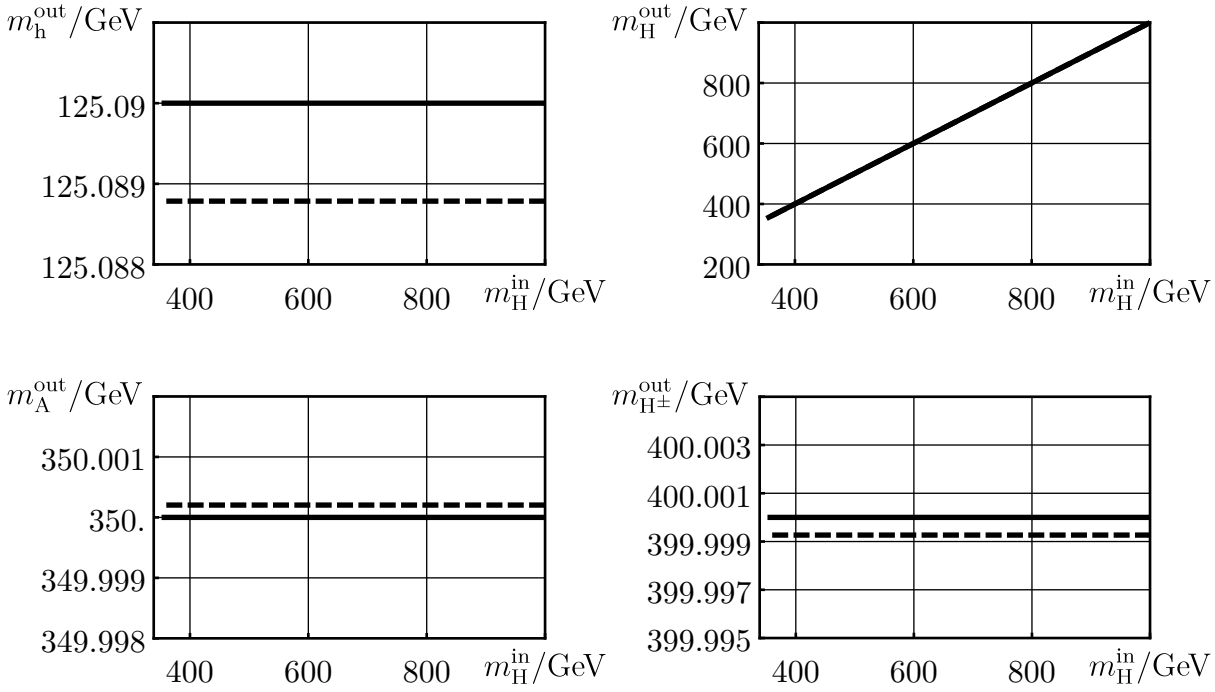

Figure 10. Tree level scan over $m_{\rm H}^{\rm in}$ with $\theta_{12} = 0$, $m_{\rm h}^{\rm in} = 125.09$ GeV, $m_{\rm A}^{\rm in} = 350$ GeV and $m_{\rm H^\pm}^{\rm in} = 400$ GeV. The solid line represents output from `FlexibleSUSY` and the dashed line is for `SPheno`. VEV's are different for the calculation of Z_{abcd} parameters in this case: 246.22 GeV for `FlexibleSUSY` and 245.6 GeV for `SPheno`. The outputs of masses are arranged as follows: Top left) lightest Higgs h, Top right) heavier scalar Higgs H, Bottom left) pseudo scalar Higgs A, and Bottom right) charged Higgs $H^\pm$.

The figure below shows the mass ratios of `FlexibleSUSY` and `SPheno`, when the vacuum expectation values are different for calculations of Z_{abcd} parameters.

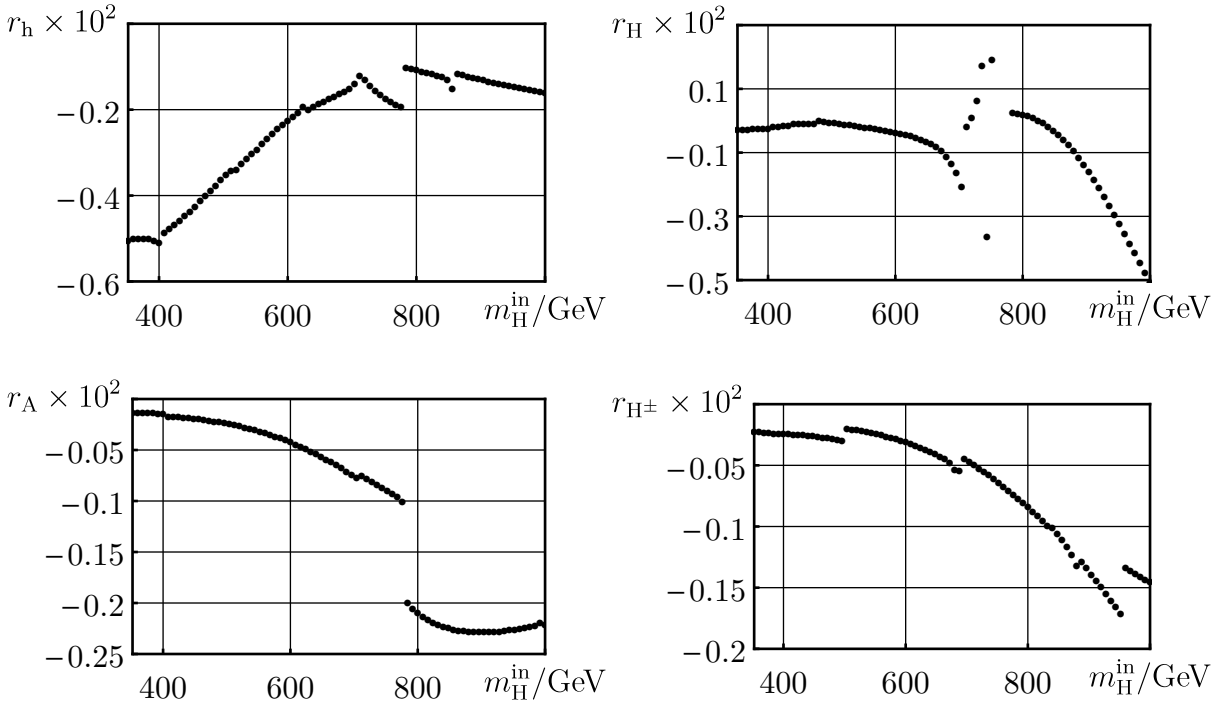

Figure 11. Higgs mass ratios r_i between `FlexibleSUSY` and `SPheno` outputs. Same parameter point and layout as specified in Fig. 10, but 1-loop corrected.

In the two following figures we show the full view of scans done over m_{H} and θ_{12} at tree level as well as with 1-loop corrections. These plots are meant to give a general idea of what the parameter space is like, since the previous plots were only cross-sections at $\theta_{12} = 0$. Because the known Z_{abcd} parameters are π-symmetric, we only scan up to π in θ_{12}.

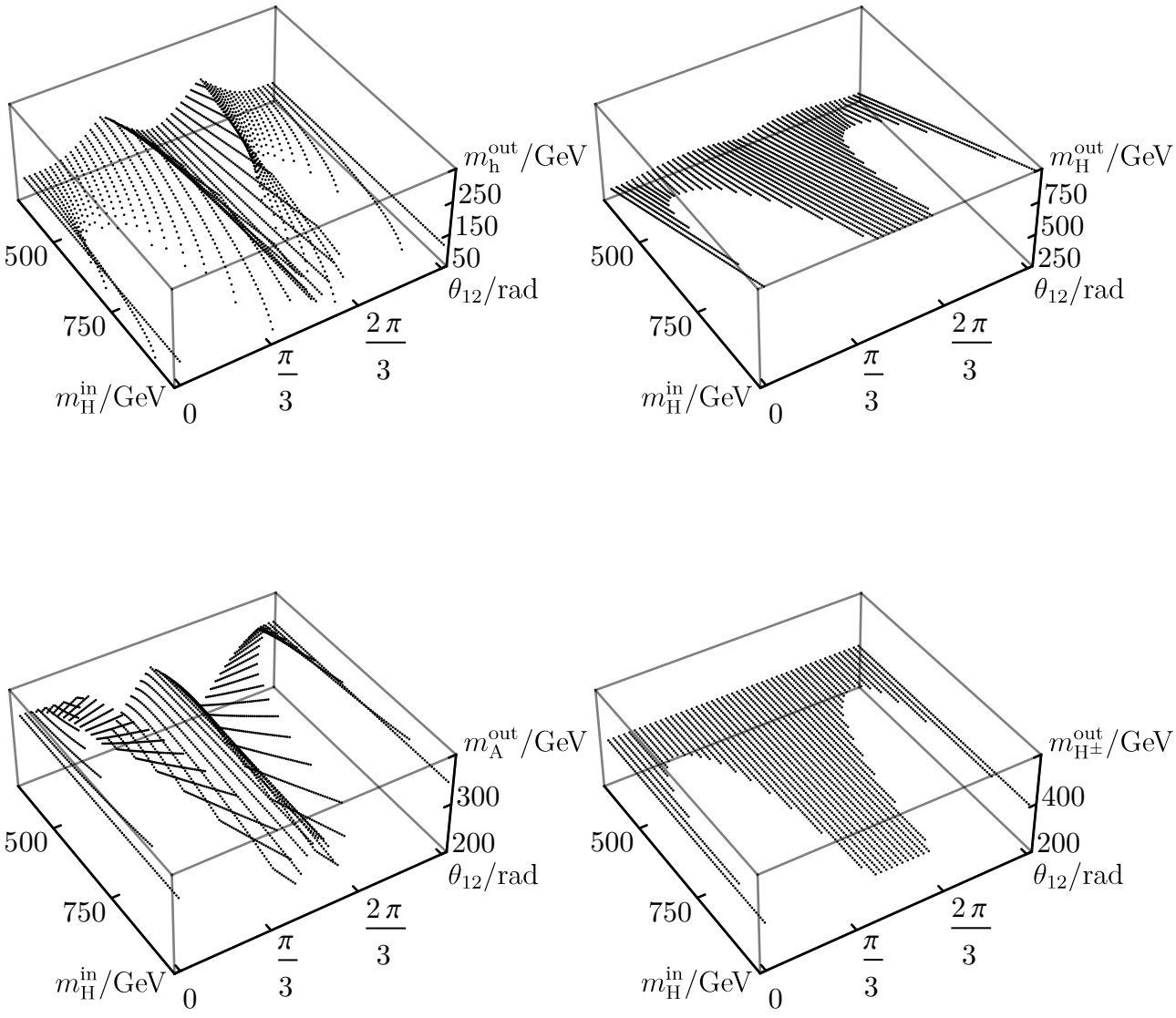

Figure 12. Tree level scan over $m_{\mathrm{H}}^{\mathrm{in}}$ and θ_{12} with $m_{\mathrm{h}}^{\mathrm{in}} = 125.09$ GeV, $m_{\mathrm{A}}^{\mathrm{in}} = 350$ GeV and $m_{\mathrm{H}^{\pm}}^{\mathrm{in}} = 400$ GeV. The outputs of masses are arranged as follows: Top left) lightest Higgs h, Top right) heavier scalar Higgs H, Bottom left) pseudo scalar Higgs A, and Bottom right) charged Higgs $H^{\pm}$. These scans were done with `FlexibleSUSY`.

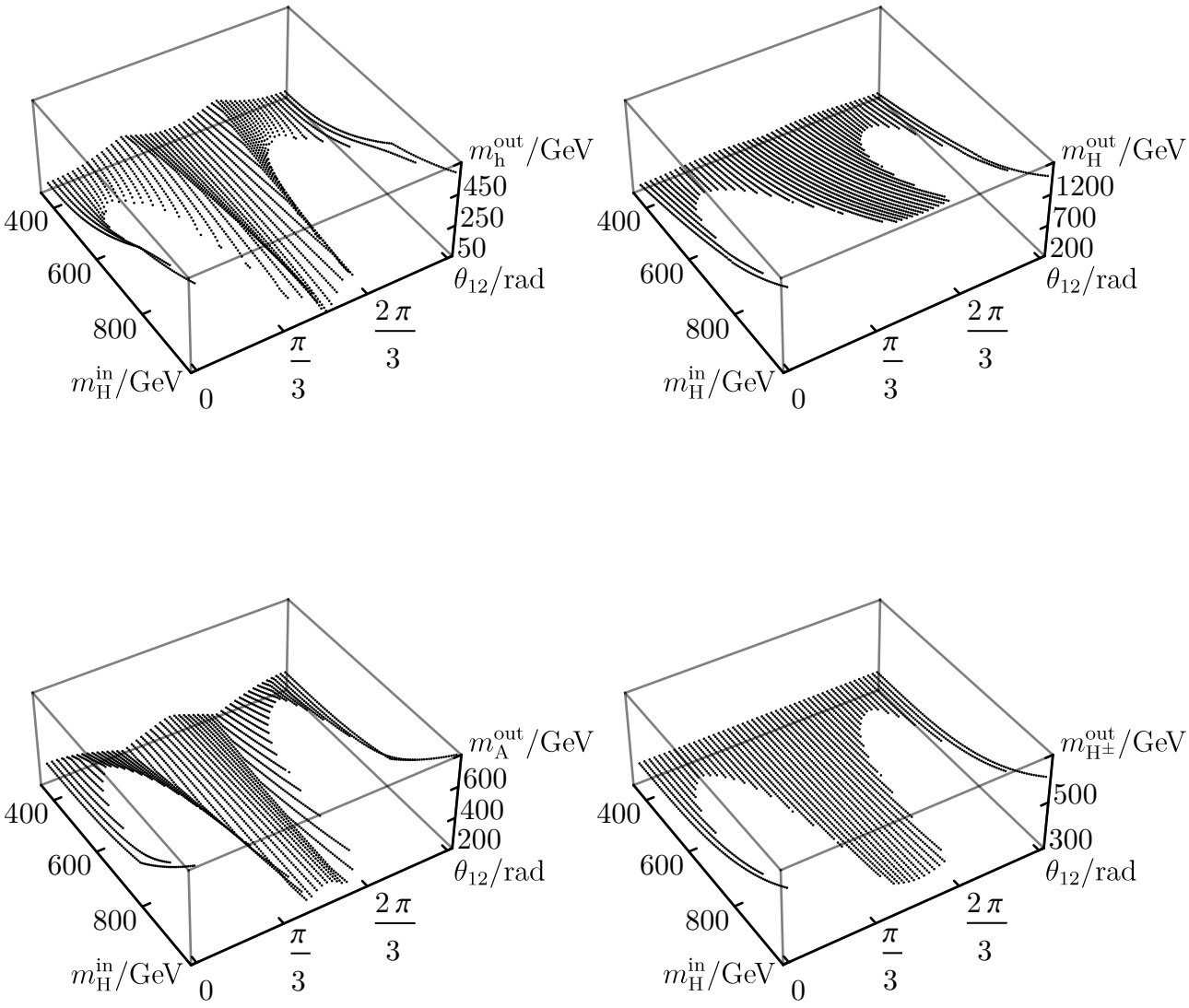

Figure 13. 1-loop corrected scan over $m_{\mathrm{H}}^{\mathrm{in}}$ and θ_{12} with $m_{\mathrm{h}}^{\mathrm{in}} = 125.09$ GeV, $m_{\mathrm{A}}^{\mathrm{in}} = 350$ GeV and $m_{\mathrm{H}^{\pm}}^{\mathrm{in}} = 400$ GeV. The outputs of masses are arranged as follows: Top left) lightest Higgs h, Top right) heavier scalar Higgs H, Bottom left) pseudo scalar Higgs A, and Bottom right) charged Higgs $H^{\pm}$. These scans were done with `FlexibleSUSY`.